

# Decays of $1^{-+}$ Charmoniumlike Hybrid

Chunjiang Shi,<sup>1,2,\*</sup> Ying Chen,<sup>1,2,†</sup> Ming Gong,<sup>1,2</sup> Xiangyu Jiang,<sup>1,2</sup> Zhaofeng Liu,<sup>1,2,3</sup> and Wei Sun<sup>1</sup>

<sup>1</sup>*Institute of High Energy Physics, Chinese Academy of Sciences, Beijing 100049, People's Republic of China*

<sup>2</sup>*School of Physical Sciences, University of Chinese Academy of Sciences, Beijing 100049, People's Republic of China*

<sup>3</sup>*Center for High Energy Physics, Peking University, Beijing 100871, People's Republic of China*

By extracting the transition amplitudes, we give the first lattice QCD prediction of the two-body decay partial widths of the  $1^{-+}$  charmoniumlike hybrid  $\eta_{c1}$ . Given the calculated mass value  $m_{\eta_{c1}} = 4.329(36)$  GeV, the  $\eta_{c1}$  decay is dominated by the open charm modes  $D_1\bar{D}$ ,  $D^*\bar{D}$  and  $D^*\bar{D}^*$  with partial widths of 258(133) MeV, 88(18) MeV and 150(118) MeV, respectively. The coupling of  $\eta_{c1}$  to  $\chi_{c1}$  plus a flavor singlet pseudoscalar is not small, but  $\chi_{c1}\eta$  decay is suppressed by the small  $\eta - \eta'$  mixing angle. The partial width of  $\eta_{c1} \rightarrow \eta_c\eta'$  is estimated to be around 1 MeV. We suggest experiments to search for  $\eta_{c1}$  in the  $P$ -wave  $D^*\bar{D}$  and  $D^*\bar{D}^*$  systems. Especially, the polarization of  $D^*\bar{D}^*$  can be used to distinguish the  $1^{-+}$  product (total spin  $S = 1$ ) from  $1^{--}$  products ( $S = 0$ ).

*Introduction.*— Quantum Chromodynamics (QCD) permits the existence of hybrid mesons that are made up of both quarks and gluons, among which the hybrid mesons with  $J^{PC} = 1^{-+}$  are most intriguing since this quantum number is prohibited for  $q\bar{q}$  states. Up to now there are three experimental candidates for  $I^G J^{PC} = 1^{-+}$  light hybrid mesons, namely,  $\pi_1(1400)$  [1],  $\pi_1(1600)$  [2–4] and  $\pi_1(2105)$  [2] (details can be found in the latest review [5] and the references therein). Recently, the BESIII collaboration reported the first observation of a  $I^G J^{PC} = 0^{+}1^{-+}$  structure  $\eta_1(1855)$  in the  $\eta\eta'$  system through the partial wave analysis of the  $J/\psi \rightarrow \gamma\eta\eta'$  process [6, 7], which is a candidate for light isoscalar  $1^{-+}$  hybrid [8–10].

It is natural to anticipate the existence of the  $1^{-+}$  charmoniumlike hybrid. There have been many lattice QCD studies predicting that the  $1^{-+}$  charmoniumlike hybrid (named  $\eta_{c1}$ ) can be the lightest with a mass  $m_{\eta_{c1}} \sim 4.3 - 4.4$  GeV [11–18]. In order to identify charmoniumlike hybrids experimentally, the theoretical prediction of their decay properties is very demanding. Phenomenological studies give a selection rule for hybrid decays that a  $q\bar{q}g$  hybrid decays preferentially into final states of an  $S$ -wave meson and a  $P$ -wave meson [19–22]. However, the  $\pi_1$  states were observed in the  $\eta\pi$ ,  $\eta'\pi$  or  $\rho\pi$  systems instead of the  $b_1\pi$  system which is expected to be the dominant decay mode. Similarly,  $\eta_1(1855)$  is observed in the  $\eta\eta'$  system. These facts indicate that there may be features of hybrid decays that have not been covered by previous phenomenological studies. Therefore, an *ab initio* investigation of the hybrid decay is desirable.

The two-body decay  $\eta_{c1} \rightarrow AB$  includes closed-charm decays  $\chi_{c1}\eta(\eta')$ ,  $\eta_c\eta(\eta')$ ,  $J/\psi\omega(\phi)$ , and open-charm modes  $D_{(s)}^*\bar{D}_{(s)}$ ,  $D_{(s)}^*\bar{D}_{(s)}^*$ ,  $D\bar{D}_1(2420)$ , etc. The effective Lagrangian for closed-charm decays can be written as

$$\begin{aligned} \mathcal{L}_1^{\text{cc}} \sim & -g_{\chi\eta}m_H H_\mu A^\mu \eta - ig_{\eta_c\eta} H_\mu \eta_c \overleftrightarrow{\partial}^\mu \eta \\ & + iH_\mu \left( g\psi_\nu \partial^\nu \omega^\mu + g'\omega_\nu \partial^\nu \psi^\mu + g_0\psi_\nu \overleftrightarrow{\partial}^\mu \omega^\nu \right), \end{aligned} \quad (1)$$

where  $\overleftrightarrow{\partial}$  represents  $\overleftarrow{\partial} - \overrightarrow{\partial}$ , and the fields  $H_\mu$ ,  $\chi_\mu$ ,  $\eta_c$ ,  $\eta$ ,  $\psi_\mu$  and  $\omega_\mu$  are for  $\eta_{c1}$ ,  $\chi_{c1}$ ,  $\eta_c$ ,  $\eta(\eta')$ ,  $J/\psi$  and  $\omega$  mesons, respectively.

For open-charm decays, the quantum number  $I^G J^{PC} = 0^{+}1^{-+}$  of  $\eta_{c1}$  requires the flavor structure of the  $D\bar{D}'(D'$  here refers to either  $D^*$  and  $D_1)$  final state to be

$$\begin{aligned} |D\bar{D}'\rangle_{(C=+)}^{(I=0)} &= \frac{1}{2} \left( |D^+D'^-\rangle + |D^0\bar{D}'^0\rangle \right) \\ &\pm \frac{1}{2} \left( |D^-D'^+\rangle + |\bar{D}^0D'^0\rangle \right) \end{aligned} \quad (2)$$

where the  $\pm$  sign stands for  $D' = D_1$  or  $D^*$ , respectively (We take the conventions  $\mathcal{C}|D\rangle = +|\bar{D}\rangle$ ,  $\mathcal{C}|D^*\rangle = -|\bar{D}^*\rangle$ ,  $\mathcal{C}|D_1\rangle = +|\bar{D}_1\rangle$ , where  $\mathcal{C}$  is the charge conjugate transformation). Similarly for the  $D^*\bar{D}^*$  system, one has

$$|D^*\bar{D}^*\rangle_{(C=+)}^{(I=0)} = \frac{1}{\sqrt{2}} \left( |D^{*+}D^{*-}\rangle + |D^{*0}\bar{D}^{*0}\rangle \right)_{(L=1)}^{(S=1)} \quad (3)$$

with the relative momentum  $L = 1$  and the total spin  $S = 1$ . When the isospin doublet fields  $D_{1\mu}$ ,  $D_\mu$  and  $D$  are introduced for  $D_1$ ,  $D^*$  and  $D$  mesons of the flavor wave functions  $(|c\bar{d}\rangle, -|c\bar{u}\rangle)^T$ , the effective Lagrangian for open-charm decays reads

$$\begin{aligned} \mathcal{L}_1^{\text{oc}} \sim & g_{D_1 D} m_H H_\mu \frac{1}{2} \left( D_1^{\mu\dagger} D + D^\dagger D_1^\mu \right) \\ & + g_{D^* \bar{D}^*} H^\mu \frac{i}{\sqrt{2}} \left( D^{\nu\dagger} \partial_\nu D_\mu + \partial_\nu D_\mu^\dagger D^\nu \right) \\ & + \frac{g_{D^* \bar{D}}}{m_H} \epsilon^{\mu\nu\rho\sigma} (\partial_\mu H_\nu) \frac{1}{2} \left[ (\partial_\rho D_\sigma^\dagger) D - D^\dagger (\partial_\rho D_\sigma) \right]. \end{aligned} \quad (4)$$

So the prediction of partial decay widths depends on a reliable determination of the effective couplings  $g_{AB}$  in the effective Lagrangian. In this Letter, We pursue this goal through lattice QCD calculations.

*Formalism.*— Instead of performing a coupled channel scattering study in the Lellouch-Lüscher formalism [23] (for a recent review see Ref. [24]), we adopt the transition matrix method proposed in Refs. [25, 26], which has been successfully applied in the lattice studies

of meson decays [27–32] and also baryon decays [33, 34]. The results for  $\Delta \rightarrow N\pi$  obtained in this method are in agreement with the physical values [35, 36] and with those from the Lellouch-Lüscher method [37–39].

According to the effective Lagrangian Eq. (1) and Eq. (4), the tree-level transition amplitudes  $x_{AB}^{(\lambda'\lambda'')\lambda} \approx \langle AB; (\lambda'\lambda''), \vec{k} | \hat{H} | \eta_{c1}, \lambda \rangle$  in the rest frame of  $\eta_{c1}$  are expressed explicitly as

$$\begin{aligned} x_{AP}^{\lambda\lambda} &= g_{AP} m_H \vec{\epsilon}_\lambda(\vec{0}) \cdot \vec{\epsilon}_{\lambda'}^*(\vec{k}), \\ x_{PP}^{\lambda\lambda} &= 2g_{PP} \vec{\epsilon}_\lambda(\vec{0}) \cdot \vec{k}, \\ x_{D^*\bar{D}}^{\lambda\lambda} &= g_{D^*\bar{D}} \vec{\epsilon}_\lambda(\vec{0}) \cdot (\vec{\epsilon}_{\lambda'}^*(\vec{k}) \times \vec{k}), \\ x_{D^*\bar{D}^*}^{\lambda\lambda''\lambda} &= 2g_{D^*\bar{D}^*} \vec{\epsilon}_\lambda(\vec{0}) \cdot \left( \vec{k} \times \left[ \vec{\epsilon}_{\lambda'}^*(\vec{k}) \times \vec{\epsilon}_{\lambda''}^*(-\vec{k}) \right] \right), \end{aligned} \quad (5)$$

where  $\epsilon_\lambda^\mu(\vec{0})$ ,  $\epsilon_{\lambda'}(\vec{k})$  and  $\epsilon_{\lambda''}(-\vec{k})$  are the polarization vectors of  $\eta_{c1}$ ,  $A$  (if a (an axial) vector) and  $B$  (if a (an axial) vector). The  $J/\psi\omega$  decay is strongly suppressed due to the OZI rule and will not be discussed in depth in this Letter, so the explicit expression of  $x_{J/\psi\omega}$  is omitted here.

On the lattice, the transition amplitude  $x_{AB}$  for  $\eta_{c1} \rightarrow AB$  appears in the temporal transfer matrix  $\hat{T} = e^{-a_t \hat{H}}$ , where  $a_t$  is the lattice spacing in the time direction. If the coupled channel effect is tentatively ignored,  $\hat{T}$  is parameterized as

$$\hat{T} = e^{-a_t \hat{H}} = e^{-a_t \bar{E}} \begin{pmatrix} e^{-a_t \Delta/2} & a_t x_{AB} \\ a_t x_{AB} & e^{+a_t \Delta/2} \end{pmatrix} \quad (6)$$

in the Hilbert space spanned by  $|\eta_{c1}\rangle$  and  $|AB\rangle$  (normalized as  $\langle \eta_{c1} | \eta_{c1} \rangle = 1$  and  $\langle AB | AB \rangle = 1$ ), where  $\bar{E} = (m_{\eta_{c1}} + E_{AB})/2$  and  $\Delta = m_{\eta_{c1}} - E_{AB}$  have been defined with  $E_{AB} = E_A + E_B$ . It is easy to show that, when each single particle state  $|X\rangle$  is normalized as  $\langle X | X \rangle = 2E_X L^3$  with  $L^3$  being the spatial volume of the lattice and  $E_X$  being the energy of  $|X\rangle$ , then  $x_{AB}^{(\lambda'\lambda'')\lambda}$  is encoded in the following ratio function [27, 28, 34, 40],

$$\begin{aligned} R_{AB}(\vec{k}, t) &= \frac{C_{AB, \eta_{c1}}^{33}(\vec{k}, t)}{\sqrt{[C_{AA}(\vec{k}, t) C_{BB}(-\vec{k}, t)]^{33} C_{\eta_{c1}, \eta_{c1}}^{33}(\vec{0}, t)}} \\ &\approx t \left( 1 + \frac{1}{24} (a_t \Delta t)^2 \right) \frac{1}{\sqrt{8L^3 m_{\eta_{c1}} E_A E_B}} \\ &\times \sum_{\lambda(\lambda'\lambda'')} \frac{a_t x_{AB}^{(\lambda'\lambda'')\lambda} [\epsilon_{(\lambda'\lambda'')}^3(\vec{k}, AB) \epsilon_{\lambda'}^{3,*}(\vec{0})]}{\sqrt{\mathcal{P}_A(\vec{k}) \mathcal{P}_B(-\vec{k}) \mathcal{P}_{\eta_{c1}}^{33}(\vec{0})}}, \end{aligned} \quad (7)$$

for  $a_t \Delta \ll 1$ , where  $C_{AB, \eta_{c1}}^{ii}(\vec{k}, t)$  is the correlation function of operators  $\mathcal{O}_{\eta_{c1}}^i$  and  $\mathcal{O}_{AB}^i(\vec{k})$  that create (or annihilate) the states  $\eta_{c1}$  and  $A(\vec{k})B(-\vec{k})$  respectively, and  $C_{XX}(\vec{p}, t)$  is the correlation function for  $X$  moving with a momentum  $\vec{p}$ . Here  $X$  refers to  $\eta_{c1}$ ,  $A$  or  $B$ . The polarization of the  $AB$  state,  $\epsilon_{(\lambda'\lambda'')}^\mu(\vec{k}, AB)$ , depends on the wave functions of  $A$  (either 1 or  $\epsilon_{\lambda'}(\vec{k})$ ) and  $B$  (either 1 or  $\epsilon_{\lambda''}(-\vec{k})$ ), as well as the relative

TABLE I. Parameters of the gauge ensembles.  $N_V$  is the number of the eigenvectors that span the Laplacian Heaviside subspace [41].

IE	$N_s^3 \times N_t$	$\beta$	$a_t^{-1}(\text{GeV})$	$\xi$	$m_\pi(\text{MeV})$	$N_V$	$N_{\text{cfg}}$
L16	$16^3 \times 128$	2.0	6.894(51)	$\sim 5.3$	$\sim 350$	70	708
L24	$24^3 \times 192$	2.0	6.894(51)	$\sim 5.3$	$\sim 350$	160	171

momentum  $\vec{k}$  (see Ref. [40] for the explicit expressions). The quantity  $\mathcal{P}_X(\vec{k})$  comes from the completeness of polarization vectors of  $X$  and takes the value of unity for a pseudoscalar and  $\mathcal{P}_X^{ij} = \delta^{ij} + \frac{k^i k^j}{m_X^2}$  for a vector. Note that the major assumptions in the derivation of Eq. (7) are

$$\langle 0 | \mathcal{O}_{\eta_{c1}} | AB \rangle \approx 0, \quad \langle 0 | \mathcal{O}_{AB} | \eta_{c1} \rangle \approx 0. \quad (8)$$

This can be checked by looking at the deviation of  $R_{AB}(\vec{0}, t=0)$  from zero.

Obviously,  $R_{AB}(t)$  in Eq. (7) is linear in the  $t$  window, where excited state contamination is negligible and  $a_t \Delta t$  is sufficiently small. This allows the transition matrix  $a_t x_{AB}^{(\lambda'\lambda'')\lambda}$ , and thereby the effective coupling  $g_{AB}$ , can be extracted from the slope of  $R_{AB}(t)$ .

*Numerical details.*— The calculations are performed on two  $N_f = 2$  gauge ensembles at the same pion mass  $m_\pi \approx 350$  MeV, the same temporal lattice spacing  $a_t$ , but with different lattice sizes, namely,  $N_s^3 \times N_t = 16^3 \times 128$  and  $24^3 \times 192$  (labeled as L16 and L24, respectively). Both ensembles are generated on anisotropic lattice with the same aspect ratio  $\xi = a_s/a_t = 5.3$  ( $a_s$  is the lattice spacing in spatial directions) [43]. The parameters of the gauge ensembles are collected in Table I. We adopt the clover fermion action in Ref. [44] for the valence charm quark and set the charm quark mass parameter by  $(m_{\eta_c} + 3m_{J/\psi})/4 = 3069$  MeV. Within the framework of the distillation method, the perambulators of light  $u, d$  quarks and charm quark are calculated with the time sources running over all the time slices and the number of eigenvectors spanning the Laplacian Heaviside subspace are chosen to be  $N_V = 70$  for L16 and  $N_V = 160$  for L24. Since all the mesons involved in  $\eta_{c1}$  decays are the ground states in specific  $J^{PC}$  channels, and the distillation method provides an inherent smearing scheme for quark fields, we use only the simplest generic quark bilinear operators for all the mesons. Table II lists the masses of mesons involved in this calculation. Since we work in the  $N_f = 2$  QCD, we label the flavor singlet (isoscalar) pseudoscalar meson by  $\eta_{(2)}$  to differentiate it from the physical states  $\eta$  and  $\eta'$  when we present the corresponding lattice results. We keep the name  $\omega$  for the isoscalar vector meson in our lattice setup by considering that the physical  $\omega$  meson is nearly a pure  $(u\bar{u} + d\bar{d})$  meson.

TABLE II. The masses of light hadrons, charmed mesons and charmonium on the two lattices. The PDG value of  $m_{D^{(*)}}$  is the average of masses of  $D^{(*)0}$  and  $D^{(*)+}$ .

$X$	$\omega$	$\eta_{(2)}$	$\eta_c$	$J/\psi$	$\chi_{c1}$	$D$	$D^*$	$D_1$	$\eta_{c1}$
$m_X(\text{L16})(\text{MeV})$	857(10)	715(10)	2975.0(3)	3099.1(2)	3559.8(1.7)	1882(1)	2023(1)	2423(7)	4330(21)
$m_X(\text{L24})(\text{MeV})$	845(7)	705(21)	2976.3(4)	3099.4(4)	3560.4(6.4)	1881(1)	2019(1)	2430(10)	4328(68)
$m_X(\text{PDG})(\text{MeV})$ [42]	782	547/958	2983	3097	3511	$\sim 1867$	$\sim 2008$	2420	-

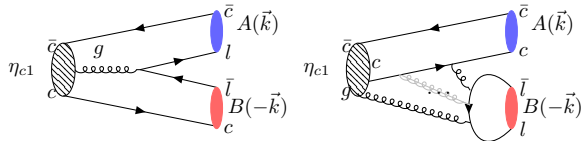


FIG. 1. Schematic diagrams illustrating the decay process  $\eta_{c1} \rightarrow AB$ . The left panel depicts the open-charm decay, while the right panel is for the closed-charm decay (at least two intermediate gluons for a light pseudoscalar and three intermediate gluons for a light vector meson in the  $AB$  system).

The key task is to calculate the correlation function  $C_{AB,\eta_{c1}}^{ii}(\vec{k}, t)$ , where both operators  $\mathcal{O}_{\eta_{c1}}^i$  and  $\mathcal{O}_{AB}^i(\vec{k})$  belong to the  $T_1$  representation of the octahedral group  $O$  on the lattice. We use the partial-wave method [45] to construct  $\mathcal{O}_{AB}^i(\vec{k})$ .  $\mathcal{O}_{\eta_{c1}}^i$  takes the generic quark bilinear form  $\epsilon_{ijk}\bar{c}\gamma_j B_k c$  with  $B_k$  being the chromomagnetic field strength. The two-particle operator  $\mathcal{O}_{AB}^i(\vec{k})$  is built by the single particle operators  $\mathcal{O}_A(\vec{k})$  and  $\mathcal{O}_B(-\vec{k})$  through a specific combination  $[\mathcal{O}_A(\vec{k}) \circ \mathcal{O}_B(-\vec{k})]^i$ , whose explicit expression is less relevant to the contents of this Letter and is given in the Supplementary Materials for Ref. [40]. When constructing the operators for open-charm systems, the flavor structures are considered according to Eq. (2) and Eq. (3). The schematic quark diagrams for the two-body  $\eta_{c1}$  decays are shown in Fig. 1 where the left panel is for the open-charm decays, in which the original gluon in  $\eta_{c1}$  splits into a light quark anti-quark pair  $l\bar{l}$ , which reorganizes with the  $c\bar{c}$  pair to form an open-charm final state. The right panel depicts the process of the closed-charm decay. Along with the  $c\bar{c}$  pair coupling to a final state charmonium, the original gluon and the gluon(s) emitted by the charm quark pair generate a flavor singlet meson (note that the mesons  $\eta(\eta'), \omega(\phi)$  have flavor singlet components). Obviously, both diagrams have annihilation diagrams of light quarks which can be readily tackled by the distillation method.

For each process  $\eta_{c1} \rightarrow A(\vec{k})B(-\vec{k})$ ,  $R_{AB}(\vec{k}, t)$  is easily derived from  $C_{AB,\eta_{c1}}^{ii}(\vec{k}, t)$  and the corresponding correlation functions of single particles. In practice, the relative momentum  $\vec{k} = 2\pi\hat{k}/L$  ( $\hat{k} = (n_1, n_2, n_3)$ ) is

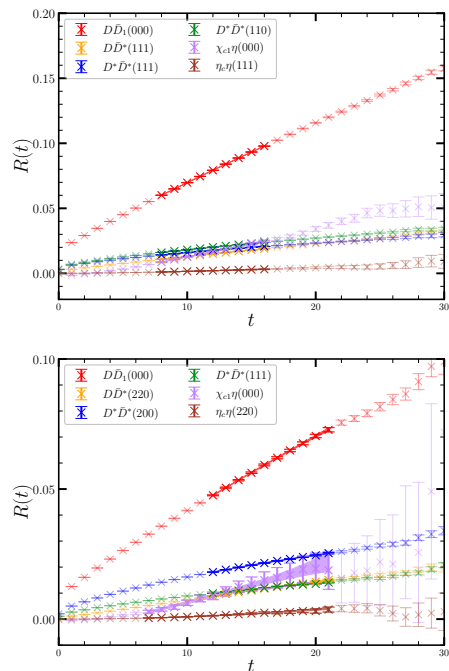


FIG. 2. The ratio function  $R_{AB}(\vec{k}, t)$  on the two gauge ensembles L16 (the upper panel) and L24 (the lower panel) for  $\eta_{c1} \rightarrow AB$ .  $AB$  refers to the decay modes  $D_1\bar{D}$ ,  $\chi_{c1}\eta_{(2)}$ ,  $D^*\bar{D}$ ,  $D^*\bar{D}^*$ ,  $\eta_c\eta_{(2)}$ . The shaded bands illustrate the fit results and the fit window using Eq. (9).

chosen so that the two-particle energy  $E_{AB}$  is as close as possible to  $m_{\eta_{c1}}$ , namely  $|a_t\Delta| \lesssim 0.01 \ll 1$ . For some channels, more than one momentum modes  $\hat{k}$  are chosen to check the momentum dependence. Figure 2 shows  $R_{AB}(t)$  for all the decay modes concerned on L16 (upper panel) and L24 (lower panel) ensembles. It can be seen that the curves of  $R_{AB}(\vec{k}, t)$  for open-charm processes and  $\chi_{c1}\eta$  exhibit clear linear behavior in the time region  $t \in [5, 20]$ . The curves of  $R_{AB}(\vec{k}, t)$  for closed-charm decays are indeed linear in  $t$  in the same time region but have much smaller slopes, which is certainly the expectation of the OZI rule. In the data analysis, we use the following function form to fit the data

$$R(t) = r_0 + r_1 t + r_3 t^3. \quad (9)$$

The shaded bands in Fig. 2 illustrate the best fit results

TABLE III. The values of  $r_1$  and  $g_{AB}$  for different decay modes ( $AB$ ) and different relative momentum modes  $\hat{k} = (n_1, n_2, n_3)$  on the two ensembles L16 and L24. The errors of the averaged  $\Gamma_{AB}$  is estimated by  $\delta g_{AB} \sim (g_{AB}^{(\max)} - g_{AB}^{(\min)})/2$ .

Mode ( $AB$ )	$\hat{k}$ (IE)	$r_1$ ( $\times 10^{-3}$ )	$g_{AB}$	$g_{AB}$ (ave.)	$\Gamma_{AB}$ (MeV)
$D_1\bar{D}$	(0, 0, 0)(L16)	4.95(5)	4.27(5)	4.6(6)	258(133)
	(0, 0, 0)(L24)	3.10(26)	4.92(41)		
$D^*\bar{D}$	(1, 1, 1)(L16)	1.11(3)	8.35(21)	8.3(7)	88(18)
	(2, 2, 0)(L24)	0.78(7)	8.34(74)		
$D^*\bar{D}^*$	(1, 1, 1)(L16)	1.00(3)	3.44(12)	4.6(1.8)	150(118)
	(1, 1, 0)(L16)	1.15(4)	3.79(12)		
	(2, 0, 0)(L24)	1.05(9)	5.06(42)		
	(1, 1, 1)(L24)	0.67(7)	6.31(58)		
$\chi_{c1}\eta(2)$	(0, 0, 0)(L16)	2.04(26)	1.31(2)	1.35(45)	-
	(0, 0, 0)(L24)	1.18(38)	1.39(45)		
$\eta_c\eta(2)$	(1, 1, 1)(L16)	0.20(6)	0.62(18)	0.55(22)	-
	(2, 2, 0)(L24)	0.10(3)	0.47(12)		

in the time windows  $[t_{\min}, t_{\max}] = [8, 18]$  for L16 and L24 ensembles. The fitted value of  $r_0$  for all the channels are few percents or even smaller and therefore justify the approximation of Eq. (8). The stability of the fit is also checked by fit in different time windows  $[t_{\min}, t_{\min} + 10]$  with  $t_{\min}$  varying from 5 to 25. It is found that, for all the channels,  $r_1$  is insensitive to the change of fit range [40]. We take  $\delta r_1 = (r_1^{(\max)} - r_1^{(\min)})/2$  of the fits with  $t_{\min} \in [6, 13]$  as a systematic error of  $r_1$  and add it to the statistical error in a quadratic way. The final result of  $r_1$  for different  $AB$  modes are listed in Table III.

For each decay mode, the connection between  $r_1$  and the transition amplitude  $x_{AB}$  can be established through Eq. (5) and Eq. (7), see the Supplementary Materials Ref. [40] for the explicit relations. Finally, on the L16 and L24 ensembles, we obtain the effective coupling  $g_{AB}$  for each decay mode  $AB$  of a specific momentum configuration  $\hat{k}$ , as shown in Table III. For each mode, the values of  $g_{AB}$  obtained on the two ensembles L16 and L24 are very close to each other and provide a self-consistent check except for  $g_{D^*\bar{D}^*}$  obtained at  $\hat{k} = (1, 1, 1)$  on L16, which deviates from other three values by roughly 40% for unknown reasons. For each decay mode  $AB$ , we average the values of  $g_{AB}$  to give our final prediction of the effective coupling  $g_{AB}$ , which is also included in Table III with the error being given by  $\delta g_{AB} \sim (g_{AB}^{(\max)} - g_{AB}^{(\min)})/2$ .

*Discussion.*— Although theoretically they are functions of meson masses, the dimensionless  $g_{AB}$  are usually assumed to be insensitive to the meson masses in the initial and final states. Consequently, the averaged  $g_{AB}$

is applied to predict the partial decay width  $\Gamma_{AB}$  of  $\eta_{c1} \rightarrow AB$  by

$$\Gamma_{AB} = \frac{1}{8\pi} \frac{k_{\text{ex}}}{m_{\eta_{c1}}^2} \overline{|\mathcal{M}(\eta_{c1} \rightarrow AB)|^2}, \quad (10)$$

where  $k_{\text{ex}}$  is the decay momentum determined by the experimental mass values of  $A$  and  $B$  along with a given  $m_{\eta_{c1}}$ ,  $\mathcal{M}$  is the tree-level decay amplitude  $x_{AB}$  in Eq. (5) with  $\vec{k}$  being replaced by  $\vec{k}_{\text{ex}}$ . Using the mass  $m_{\eta_{c1}} = 4.329(36)$  GeV determined by averaging the values on two ensembles, the partial widths  $\Gamma_{AB}$  of all the decay modes concerned are predicted and are shown in Table III. Specifically, the partial widths of open charm decays at  $m_{\eta_{c1}} = 4.329(36)$  GeV are

$$\begin{aligned} \Gamma_{D_1\bar{D}} &= 258(133) \text{ MeV}, \\ \Gamma_{D^*\bar{D}^*} &= 150(118) \text{ MeV}, \\ \Gamma_{D^*\bar{D}} &= 88(18) \text{ MeV}, \end{aligned} \quad (11)$$

which indicate  $\eta_{c1}$  is a very wide resonance with a total width  $\Gamma_{\eta_{c1}} \gtrsim 400$  MeV. The  $D_1\bar{D}$  dominance of the  $\eta_{c1}$  decay is in agreement with the expectation of the flux tube model qualitatively, which favors the final state of a  $S$ -wave meson and a  $P$ -wave meson a hybrid state. However, the partial width in this study is much larger than  $\sim 25$  MeV predicted by the flux tube model [22]. On the other hand, the  $D_1\bar{D}$  mass threshold  $E_{\text{th}}(D_1\bar{D}) \approx 4290$  MeV is very close to the expected  $\eta_{c1}$  mass, so the partial width  $\Gamma_{D_1\bar{D}}$  is very sensitive to the  $m_{\eta_{c1}}$ . There is a possibility that this decay mode is kinetically prohibited if  $m_{\eta_{c1}} < E_{\text{th}}(D_1\bar{D})$ .

It is most striking that the  $D^*\bar{D}^*$  and  $D^*\bar{D}$  decays have large branching fractions and even dominate the  $\eta_{c1}$  decay when  $m_{\eta_{c1}} < E_{\text{th}}(D\bar{D}_1)$ . The large  $\Gamma_{D^*\bar{D}^*}$  and  $\Gamma_{D^*\bar{D}}$  refute the expectation of the flux tube model that the decay modes of two  $S$ -wave mesons are disfavored and that decay modes with two spatially identical particles such as  $D^*\bar{D}^*$  is prohibited [19–22]. Our observation suggests  $D^*\bar{D}$  and  $D^*\bar{D}^*$  are good channels for  $\eta_{c1}$  to be searched experimentally. First, the  $D^*\bar{D}$  and  $D^*\bar{D}^*$  decay modes are kinetically favored since their thresholds are much lower than the expected  $m_{\eta_{c1}}$ . Secondly,  $D$  and  $D^*$  are easier to be reconstructed than  $D_1$  in experiments. One feature of the  $D^*\bar{D}^*$  channel is that, its  $C$ -parity can be determined by measuring the polarizations of  $D^*$  and  $\bar{D}^*$ , since the  $C$ -parity of a  $P$ -wave  $D^*\bar{D}^*$  system is determined by its total spin  $S$ . This feature can be used to distinguish the possible  $1^{-+}$  state from the  $1^{--}$  states in the  $D^*\bar{D}^*$  system.

For the closed charm decay modes, the tiny partial width of the  $J/\psi\omega$  decay is understood due to the OZI rule. However, the effective couplings for the  $\chi_{c1}\eta(2)$  and  $\eta_c\eta(2)$  decays appear not to be particularly small. This can be attributed to the enhancement by the QCD  $U_A(1)$  anomaly [46, 47], which introduces an

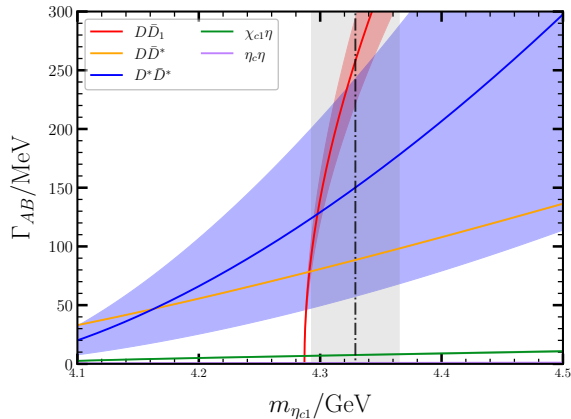


FIG. 3. The  $m_{\eta_{c1}}$  dependence of the partial decay widths. The vertical dashed line and the grey band illustrate the lattice result of  $m_{\eta_{c1}}$  with errors, and the colored bands show the partial decay widths varying with respect to  $m_{\eta_{c1}}$  in the range from 4.1 to 4.5 GeV. The mixing angle  $\theta = -24.5^\circ$  from the linear mass relation [42] is used to estimate the partial decay widths of  $\chi_{c1}\eta$ ,  $\eta_c\eta'$  decay modes.

anomalous coupling between gluons and the flavor singlet pseudoscalar meson (the isoscalar  $\eta_{(2)}$  in the  $N_f = 2$  case). Since this coupling is proportional to  $\sqrt{N_f}$ , the coupling  $g_{AB}$  for  $\chi_{c1}\eta_{(2)}$  and  $\eta_c\eta_{(2)}$  in Table III should be proportionally increased by a factor of  $\sqrt{3/2}$  for the flavor SU(3) case. Considering that the  $\chi_{c1}\eta'$  is likely kinetically prohibited and the  $\eta_c\eta$  decay is suppressed by  $\sin^2\theta$  with  $\theta = -24.5^\circ$  (linear mass relation) or  $-11.3^\circ$  (squared mass relation) [42], where  $\theta$  is the small  $\eta - \eta'$  mixing angle, here we restrict our predictions on the partial widths of  $\chi_{c1}\eta$  and  $\eta_c\eta'$  decays as

$$\begin{aligned}\Gamma_{\chi_{c1}\eta} &= \sin^2\theta \cdot 44(29) \text{ MeV}, \\ \Gamma_{\eta_c\eta'} &= \cos^2\theta \cdot 0.93(77) \text{ MeV}.\end{aligned}\quad (12)$$

Although many systematic uncertainties are not well controlled yet, the results in this Letter have already provided very important physical information for the nature of the  $\eta_{c1}$  decay. Since the open-charm partial widths are sensitive to  $m_{\eta_{c1}}$ , we plot the  $m_{\eta_{c1}}$  dependence of the partial widths as curves with colored error bands in Fig. 3, where the vertical grey band illustrates  $m_{\eta_{c1}}$  obtained in this Letter. This figure serves as a further guidance for experiments to search for  $\eta_{c1}$ . In comparison with  $e^+e^-$  colliders that favor the production of  $1^{--}$  mesons, the  $B$  meson decay might be a good place to search for the  $\eta_{c1}$  search. The LHCb and Belle II experiments may take the mission.

*Summary.*— Based on two gauge ensembles of  $N_f = 2$  dynamical quarks at  $m_\pi \approx 350$  MeV, we perform the first lattice QCD calculation of the two-body partial decay widths of the  $1^{--}$  charmonium-like hybrids  $\eta_{c1}$ . We extract the decay amplitudes for open charm and

closed charm decays directly from hadronic correlation functions, and then predict the partial widths  $\Gamma_{D_1\bar{D}} = 258(133)$  MeV,  $\Gamma_{D^*\bar{D}^*} = 150(118)$  MeV and  $\Gamma_{D^*\bar{D}} = 88(18)$  MeV for  $m_{\eta_{c1}} = 4329(36)$  MeV, which indicate that  $\eta_{c1}$  is a wide resonance. The strikingly large partial widths of  $D^*\bar{D}$  and  $D^*\bar{D}^*$  decays suggest these system to be good places for the  $\eta_{c1}$  search. Especially, the polarization of the  $P$ -wave  $D^*\bar{D}^*$  is an ideal probe to distinguish the  $1^{--}$  products from  $1^{--}$  ones. LHCb, Belle II and BESIII experiments may take the mission to search for  $\eta_{c1}$  in  $D^*\bar{D}$  and  $D^*\bar{D}^*$  systems.

*Acknowledgments.*— We thank Kuang-Ta Chao, Qiang Zhao, Changzheng Yuan, Beijiang Liu and Feng-Kun Guo for valuable discussions. This work is supported by the National Key Research and Development Program of China (No. 2020YFA0406400), the Strategic Priority Research Program of Chinese Academy of Sciences (No. XDB34030302) and the National Natural Science Foundation of China (NNSFC) under Grants No. 11935017, No. 12293060, No. 12293061, No. 12293065, No. 12075253, No. 12070131001 (CRC 110 by DFG and NNSFC), No. 12175063, No. 12205311. The Chroma software system [48] and QUDA library [49, 50] are acknowledged. The computations were performed on the HPC clusters at Institute of High Energy Physics (Beijing) and China Spallation Neutron Source (Dongguan), and the ORISE computing environment.

\* shichunjiang@ihep.ac.cn

† chen@ihep.ac.cn

- [1] D. Alde *et al.* (IHEP-Brussels-Los Alamos-Annecey (LAPP)), *Phys. Lett. B* **205**, 397 (1988).
- [2] G. S. Adams *et al.* (E852), *Phys. Rev. Lett.* **81**, 5760 (1998).
- [3] M. Aghasyan *et al.* (COMPASS), *Phys. Rev. D* **98**, 092003 (2018), arXiv:1802.05913 [hep-ex].
- [4] A. Rodas *et al.* (JPAC), *Phys. Rev. Lett.* **122**, 042002 (2019), arXiv:1810.04171 [hep-ph].
- [5] H.-X. Chen, W. Chen, X. Liu, Y.-R. Liu, and S.-L. Zhu, *Rept. Prog. Phys.* **86**, 026201 (2023), arXiv:2204.02649 [hep-ph].
- [6] M. Ablikim *et al.* (BESIII), *Phys. Rev. Lett.* **129**, 192002 (2022), arXiv:2202.00621 [hep-ex].
- [7] M. Ablikim *et al.* (BESIII), *Phys. Rev. D* **106**, 072012 (2022), arXiv:2202.00623 [hep-ex].
- [8] H.-X. Chen, N. Su, and S.-L. Zhu, *Chin. Phys. Lett.* **39**, 051201 (2022), arXiv:2202.04918 [hep-ph].
- [9] L. Qiu and Q. Zhao, *Chin. Phys. C* **46**, 051001 (2022), arXiv:2202.00904 [hep-ph].
- [10] V. Shastry, C. S. Fischer, and F. Giacosa, *Phys. Lett. B* **834**, 137478 (2022), arXiv:2203.04327 [hep-ph].
- [11] X. Liao and T. Manke, (2002), arXiv:hep-lat/0210030.
- [12] Z.-H. Mei and X.-Q. Luo, *Int. J. Mod. Phys. A* **18**, 5713 (2003), arXiv:hep-lat/0206012.
- [13] J. J. Dudek and E. Rrapaj, *Phys. Rev. D* **78**, 094504 (2008), arXiv:0809.2582 [hep-ph].

- [14] J. J. Dudek, R. Edwards, and C. E. Thomas, *Phys. Rev. D* **79**, 094504 (2009), arXiv:0902.2241 [hep-ph].
- [15] L. Liu, G. Moir, M. Peardon, S. M. Ryan, C. E. Thomas, P. Vilaseca, J. J. Dudek, R. G. Edwards, B. Joo, and D. G. Richards (Hadron Spectrum), *J. High Energy Phys.* **07**, 126 (2012) (2012), arXiv:1204.5425 [hep-ph].
- [16] Y.-B. Yang, Y. Chen, G. Li, and K.-F. Liu, *Phys. Rev. D* **86**, 094511 (2012), arXiv:1202.2205 [hep-ph].
- [17] Y. Ma, W. Sun, Y. Chen, M. Gong, and Z. Liu, *Chin. Phys. C* **45**, 093111 (2021), arXiv:1910.09819 [hep-lat].
- [18] N. Brambilla, S. Eidelman, C. Hanhart, A. Nefediev, C.-P. Shen, C. E. Thomas, A. Vairo, and C.-Z. Yuan, *Phys. Rept.* **873**, 1 (2020), arXiv:1907.07583 [hep-ex].
- [19] N. Isgur and J. E. Paton, *Phys. Rev. D* **31**, 2910 (1985).
- [20] F. E. Close and P. R. Page, *Nucl. Phys. B* **443**, 233 (1995), arXiv:hep-ph/9411301.
- [21] P. R. Page, *Phys. Lett. B* **402**, 183 (1997), arXiv:hep-ph/9611375.
- [22] P. R. Page, E. S. Swanson, and A. P. Szczepaniak, *Phys. Rev. D* **59**, 034016 (1999), arXiv:hep-ph/9808346.
- [23] L. Lellouch and M. Luscher, *Commun. Math. Phys.* **219**, 31 (2001), arXiv:hep-lat/0003023.
- [24] R. A. Briceño, J. J. Dudek, and R. D. Young, *Rev. Mod. Phys.* **90**, 025001 (2018), arXiv:1706.06223 [hep-lat].
- [25] C. McNeile, C. Michael, and P. Pennanen (UKQCD), *Phys. Rev. D* **65**, 094505 (2002), arXiv:hep-lat/0201006.
- [26] C. McNeile and C. Michael (UKQCD), *Phys. Lett. B* **556**, 177 (2003), arXiv:hep-lat/0212020.
- [27] C. McNeile, C. Michael, and G. Thompson (UKQCD), *Phys. Rev. D* **70**, 054501 (2004), arXiv:hep-lat/0404010.
- [28] C. Michael, *PoS LAT2005*, 008 (2006), arXiv:hep-lat/0509023.
- [29] C. McNeile and C. Michael (UKQCD), *Phys. Rev. D* **73**, 074506 (2006), arXiv:hep-lat/0603007.
- [30] C. McNeile and C. Michael (UKQCD), *Phys. Rev. D* **74**, 014508 (2006), arXiv:hep-lat/0604009.
- [31] A. Hart, C. McNeile, C. Michael, and J. Pickavance (UKQCD), *Phys. Rev. D* **74**, 114504 (2006), arXiv:hep-lat/0608026.
- [32] C. Michael, *Eur. Phys. J. A* **31**, 793 (2007), arXiv:hep-lat/0609008.
- [33] C. Alexandrou, J. W. Negele, M. Petschlies, A. Strelchenko, and A. Tsapalis, *Phys. Rev. D* **88**, 031501 (2013), arXiv:1305.6081 [hep-lat].
- [34] C. Alexandrou, J. W. Negele, M. Petschlies, A. V. Pochinsky, and S. N. Syritsyn, *Phys. Rev. D* **93**, 114515 (2016), arXiv:1507.02724 [hep-lat].
- [35] V. Pascalutsa and M. Vanderhaeghen, *Phys. Rev. D* **73**, 034003 (2006), arXiv:hep-ph/0512244.
- [36] T. R. Hemmert, B. R. Holstein, and N. C. Mukhopadhyay, *Phys. Rev. D* **51**, 158 (1995), arXiv:hep-ph/9409323.
- [37] C. W. Andersen, J. Bulava, B. Hörz, and C. Morningstar, *Phys. Rev. D* **97**, 014506 (2018), arXiv:1710.01557 [hep-lat].
- [38] G. Silvi *et al.*, *Phys. Rev. D* **103**, 094508 (2021), arXiv:2101.00689 [hep-lat].
- [39] C. Morningstar, J. Bulava, A. D. Hanlon, B. Hörz, D. Mohler, A. Nicholson, S. Skinner, and A. Walker-Loud, *PoS LATTICE2021*, 170 (2022), arXiv:2111.07755 [hep-lat].
- [40] See the Supplemental Material that presents the details of the formula derivations and the operator constructions.
- [41] M. Peardon, J. Bulava, J. Foley, C. Morningstar, J. Dudek, R. G. Edwards, B. Joo, H.-W. Lin, D. G. Richards, and K. J. Juge (Hadron Spectrum), *Phys. Rev. D* **80**, 054506 (2009), arXiv:0905.2160 [hep-lat].
- [42] R. L. Workman *et al.* (Particle Data Group), *PTEP* **2022**, 083C01 (2022).
- [43] X. Jiang, W. Sun, F. Chen, Y. Chen, M. Gong, Z. Liu, and R. Zhang, (2022), arXiv:2205.12541 [hep-lat].
- [44] G.-Z. Meng *et al.* (CLQCD), *Phys. Rev. D* **80**, 034503 (2009), arXiv:0905.0752 [hep-lat].
- [45] S. Prelovsek, U. Skerbis, and C. B. Lang, *JHEP* **01**, 129 (2017), arXiv:1607.06738 [hep-lat].
- [46] X. Jiang, F. Chen, Y. Chen, M. Gong, N. Li, Z. Liu, W. Sun, and R. Zhang, *Phys. Rev. Lett.* **130**, 061901 (2023), arXiv:2206.02724 [hep-lat].
- [47] G. S. Bali, S. Collins, S. Dürr, and I. Kanamori, *Phys. Rev. D* **91**, 014503 (2015), arXiv:1406.5449 [hep-lat].
- [48] R. G. Edwards and B. Joo (SciDAC, LHPC, UKQCD), *Nucl. Phys. B Proc. Suppl.* **140**, 832 (2005), arXiv:hep-lat/0409003.
- [49] M. A. Clark, R. Babich, K. Barros, R. C. Brower, and C. Rebbi, *Comput. Phys. Commun.* **181**, 1517 (2010), arXiv:0911.3191 [hep-lat].
- [50] R. Babich, M. A. Clark, B. Joo, G. Shi, R. C. Brower, and S. Gottlieb, in *SC11 International Conference for High Performance Computing, Networking, Storage and Analysis* (2011) arXiv:1109.2935 [hep-lat].

## SUPPLEMENTARY MATERIALS

These supplemental materials provide further information on our study on the partial decay widths of the  $1^{-+}$  charmoniumlike hybrid  $\eta_{c1}$ . We present the details on the parametrization of the correlation function  $C_{AB,\eta_{c1}}^{ij}$  and show how the related transition amplitude is encoded. We also give a description of our data analysis in extracting the amplitudes to justify the reliability of the numerical results. The procedure of the meson-meson operators with the specific quantum numbers  $I^G J^{PC}$  follows the established method, so we put it in the first part for further reference.

### S1. Meson-meson operators

We use the partial-wave method to construct the interpolating meson-meson (labeled as  $A$  and  $B$ ) operators for the specific quantum numbers  $J^P$ . In general, let  $\mathcal{O}_X^{M_X}(\vec{k})$  be the operator for the particle  $X = A$  or  $B$  with spin  $S_X$  and spin projection  $M_X$  in the  $z$ -direction, then for the total angular momentum  $J$  and the  $z$ -axis projection  $M$ , the relative orbital angular momentum  $L$ , the total spin  $S$ , the explicit construction of the  $AB$  operator is expressed as

$$\begin{aligned} \mathcal{O}_{AB;JLSP}^M(\hat{k}) &= \sum_{M_L, M_S, M_A, M_B} \langle L, M_L; S, M_S | JM \rangle \langle S_A M_A; S_B M_B | S, M_S \rangle \\ &\times \sum_{R \in O_h} Y_{LM_L}^*(R \circ \vec{k}) \mathcal{O}_A^{M_A}(R \circ \vec{k}) \mathcal{O}_B^{M_B}(-R \circ \vec{k}), \end{aligned} \quad (\text{S1})$$

where  $\hat{k} = (n_1, n_2, n_3)$  is the momentum mode of  $\vec{k} = \frac{2\pi}{L a_s} \hat{k}$  with  $n_1 \geq n_2 \geq n_3 \geq 0$  by convention,  $R \circ \vec{k}$  is the spatial momentum rotated from  $\vec{k}$  by  $R \in O_h$  with  $O_h$  being the lattice symmetry group,  $|S, M_S\rangle$  is the total spin state of the two particles involved,  $|LM_L\rangle$  is the relative orbital angular momentum state, and  $|JM\rangle$  is the total angular momentum state, and  $Y_{LM_L}^*(R \circ \vec{k})$  is the spherical harmonic function of the direction of  $R \circ \vec{k}$ .

For the case of this study,  $\eta_{c1}$  has quantum numbers  $I^G J^{PC} = 0^+ 1^{-+}$ . So we need the two-meson operators of  $J^P = 1^-$ , which can be deduced from the  $T_1^P$  representation of  $O_h$ . The two-body decays of  $\eta_{c1}$  include the  $S$ -wave decay  $AP$  (one axial vector meson and one pseudoscalar meson), the  $P$ -wave  $PP$  mode (two pseudoscalars), the  $P$ -wave  $VP$  mode (one vector and one pseudoscalar), and the  $P$ -wave  $VV$  mode. For closed-charm decays, such as  $\chi_{c1}\eta(\eta')$  ( $AP$ ),  $\eta_c\eta(\eta')$  and  $J/\psi\omega(\phi)$ , the  $\mathcal{C}$ -parity of the two meson system is definitely the product of those of the constituent mesons. For open-charm decays such as  $D_1\bar{D}$ ,  $D^*\bar{D}$ , the flavor structure of the  $D\bar{D}'$  ( $D'$  here refers to either  $D^*$  and  $D_1$ ) final state should be

$$|D\bar{D}'\rangle_{(C=+)}^{(I=0)} = \frac{1}{2} \left( |D^+ D'^-\rangle + |D^0 \bar{D}'^0\rangle \right) \pm \frac{1}{2} \left( |D^- D'^+\rangle + |\bar{D}^0 D'^0\rangle \right) \quad (\text{S2})$$

where the  $\pm$  sign stands for  $D' = D_1$  or  $D^*$ , respectively (We take the conventions  $\mathcal{C}|D\rangle = +|\bar{D}\rangle$ ,  $\mathcal{C}|D^*\rangle = -|\bar{D}^*\rangle$ ,  $\mathcal{C}|D_1\rangle = +|\bar{D}_1\rangle$ , where  $\mathcal{C}$  is the charge conjugate transformation). For the  $D^*\bar{D}^*$  decay, the  $\mathcal{C}$ -parity  $C = +$  requires  $L + S = \text{even}$ , such that the flavor structure of the state is

$$|D^*\bar{D}^*\rangle_{(C=+)}^{(I=0)} = \frac{1}{\sqrt{2}} \left( |D^{*+} D^{*-}\rangle + |D^{*0} \bar{D}^{*0}\rangle \right)_{(L=1)}^{(S=1)} \quad (\text{S3})$$

with the relative momentum  $L = 1$  and the total spin  $S = 1$ .

These flavor structures are taken into account both in the construction the two-meson operators and in the calculation of correlation functions. Now we consider the concrete spatial structure of the required two-meson operators. Since the quantum numbers  $J, L, S, P$  are perfectly known for each decay mode, we name the two-meson operator by  $\mathcal{O}_{AB}^M$  and omit the  $JLSP$  subscripts in the following discussions and expressions. On the other hand, it is known that the  $1^-$  ( $T_1^-$ ) operator has three components labeled by  $i = 1, 2, 3$  (corresponding to  $x, y, z$  components, respectively). In practice, we use the third component ( $i = 3$ ) which corresponds to the  $M = 0$  case in Eq. (S1).

The operators for the  $AP$  mode ( $D_1\bar{D}$  and  $\chi_{c1}\eta_{(2)}$ ) are very simple. Here  $\eta_{(2)}$  refers to the isoscalar pseudoscalar meson in the  $N_f = 2$  lattice QCD. Since the two mesons are in  $S$ -wave and both the  $D_1\bar{D}$  and  $\chi_{c1}\eta_{(2)}$  thresholds are very close to  $m_{\eta_{c1}}$ , so we choose the momentum mode  $\hat{k} = (0, 0, 0)$ . On the other hand, we abbreviate the single meson operators by  $A$  and  $P$ , respectively, in the explicit expressions of two-meson operators. This convention applies also for other decay modes. For the quantum numbers ( $T_1^+$ ,  $J = 1, L = 0, S = 1, \hat{k} = (0, 0, 0)$ ), the operator is

$$\mathcal{O}_{AP}^3(0) = A^3(\vec{0})P(\vec{0}). \quad (\text{S4})$$

Here we omit the constant factor  $1/\sqrt{4\pi}$  that comes from  $Y_{00}$ . Actually for the momentum modes and the spin configurations involved in this work, the Clebsch-Gordan coefficients and the spherical harmonic functions result in the relative signs between different terms of a two-meson operator  $\mathcal{O}_A B^3(\hat{k})$  apart from an overall constant factor. Since this constant factor can be cancelled out by taking a proper ratio of correlation functions and therefore is irrelevant to the physical results, we omit it throughout the construction of two-meson operators.

The  $VP$  mode is in  $P$ -wave and has only one particle composition, namely,  $D^* \bar{D}$ . The two mesons in  $P$ -wave have nonzero relative momentum. Since the momentum modes involved in this study are  $\hat{k} = (n, 0, 0), (n, n, 0), (n, n, n)$  types, the different orientations of the relative momentum are reflected by the signs of its nonzero components. So we introduce three subscripts, which are different combinations of  $+, -, 0$ , to the single meson operators. For example,  $V_{+-0}^3$  means the third component of the operator for a vector meson of momentum  $\vec{k} = \frac{2\pi}{La_s}(n, -n, 0)$ . Thus for the momentum mode  $\hat{k} = (1, 0, 0)$ , the  $\mathcal{O}_{VP}$  operator of quantum number  $(T_1^-, J = 1, L = 1, S = 1)$  has four terms,

$$\mathcal{O}_{VP}^3 = +V_{0+0}^1 P_{0-0} - V_{0-0}^1 P_{0+0} - V_{+00}^2 P_{-00} + V_{-00}^2 P_{+00}. \quad (\text{S5})$$

In practice, we choose the momentum mode  $\hat{k} = (1, 1, 1)$  on the L16 ensemble and  $\hat{k} = (2, 2, 0)$  on the L24 ensemble, which make the energies of  $D^* \bar{D}$  very close to  $m_{\eta_{c1}}$ . The explicit expression of  $\mathcal{O}_{VP}^3$  of quantum numbers  $(T_1^-, J = 1, L = 1, S = 1)$  for  $\hat{k} = (2, 2, 0)$  is

$$\begin{aligned} \mathcal{O}_{VP}^3 = & +V_{+++}^1 P_{---} + V_{+-+}^1 P_{--+} + V_{0++}^1 P_{0--} + V_{0+-}^1 P_{0-+} \\ & - V_{-+0}^1 P_{+0+} - V_{-+0}^1 P_{+0-} - V_{0--}^1 P_{0++} - V_{0-+}^1 P_{0+-} \\ & + V_{-+0}^2 P_{+0+} + V_{-+0}^2 P_{+0-} + V_{-0+}^2 P_{+0-} + V_{-+0}^2 P_{+0-} \\ & - V_{+++}^2 P_{---} - V_{++0}^2 P_{-0-} - V_{+0-}^2 P_{-0+} - V_{+0-}^2 P_{-+0}. \end{aligned} \quad (\text{S6})$$

For  $\hat{k} = (1, 1, 1)$ , one has

$$\begin{aligned} \mathcal{O}_{VP}^3 = & +V_{+++}^1 P_{---} + V_{+-+}^1 P_{--+} + V_{-+-}^1 P_{+-+} + V_{-++}^1 P_{+--} \\ & - V_{-+0}^1 P_{+0+} - V_{-+0}^1 P_{+0-} - V_{+0-}^1 P_{-0+} - V_{+0-}^1 P_{-0-} \\ & + V_{-+0}^2 P_{+0+} + V_{-+0}^2 P_{+0-} + V_{-0+}^2 P_{+0-} + V_{-+0}^2 P_{+0-} \\ & - V_{+++}^2 P_{---} - V_{++0}^2 P_{-0-} - V_{+0-}^2 P_{-0+} - V_{+0-}^2 P_{-+0}. \end{aligned} \quad (\text{S7})$$

Similarly,  $PP$  operators are built for  $\hat{k} = (n, 0, 0), (n, n, 0)$ , and  $(1, 1, 1)$  modes, respectively. The explicit expressions are

$$\mathcal{O}_{PP}^3 = +P_{00+} P'_{00-} - P_{00-} P'_{00+} \quad (\text{S8})$$

for  $\hat{k} = (n, 0, 0)$ ,

$$\begin{aligned} \mathcal{O}_{PP}^3 = & +P_{+++} P'_{---} - P_{+++} P'_{--+} + P_{+-+} P'_{-+-} - P_{+-+} P'_{-++} \\ & + P_{-++} P'_{+--} - P_{-++} P'_{+0-} + P_{-+0} P'_{+0-} - P_{-+0} P'_{+0+} \end{aligned} \quad (\text{S9})$$

for  $\hat{k} = (1, 1, 1)$ , and

$$\begin{aligned} \mathcal{O}_{PP}^3 = & -P_{-0-} P'_{+0+} + P_{-0+} P'_{+0-} - P_{0--} P'_{0++} + P_{0-+} P'_{0+-} \\ & - P_{0+-} P'_{0-+} + P_{0++} P'_{0--} - P_{+0-} P'_{-0+} + P_{+0+} P'_{-0-}, \end{aligned} \quad (\text{S10})$$

for  $\hat{k} = (n, n, 0)$ .

In the  $VV$  mode we only consider the open-charm  $D^* \bar{D}^*$  decay since the  $J/\psi \omega(\phi)$  decay is strongly suppressed by the OZI rule. For this particle-antiparticle pair, the  $\mathcal{C}$ -parity  $C = +$  requires  $L + S = \text{even}$ , so we construct the  $D^* \bar{D}^*$  operators of quantum numbers  $(T_1^-, J = 1, L = 1, S = 1)$ . Let  $V^i$  and  $\bar{V}^i$  be the operators for  $D^*$  and  $\bar{D}^*$ , respectively, then for the momentum mode  $\hat{k} = (n, 0, 0)$ , we have

$$\begin{aligned} \mathcal{O}_{VV}^3 = & -V_{+00}^1 \bar{V}_{-00}^3 + V_{-00}^1 \bar{V}_{+00}^3 - V_{0+0}^2 \bar{V}_{0-0}^3 + V_{0-0}^2 \bar{V}_{0+0}^3 \\ & + V_{+00}^3 \bar{V}_{-00}^1 - V_{-00}^3 \bar{V}_{+00}^1 + V_{0+0}^3 \bar{V}_{0-0}^2 - V_{0-0}^3 \bar{V}_{0+0}^2. \end{aligned} \quad (\text{S11})$$

For the momentum mode  $\hat{k} = (n, n, 0)$ , the  $VV$  operator reads,

$$\begin{aligned}
\mathcal{O}_{VV}^3 = & -V_{++0}^1 \bar{V}_{--0}^3 - V_{+0+}^1 \bar{V}_{-0-}^3 - V_{+0-}^1 \bar{V}_{-0+}^3 - V_{+-0}^1 \bar{V}_{-+0}^3 \\
& + V_{-+0}^1 \bar{V}_{+-0}^3 + V_{-0+}^1 \bar{V}_{+0-}^3 + V_{-0-}^1 \bar{V}_{+0+}^3 + V_{--0}^1 \bar{V}_{++0}^3 \\
& - V_{++0}^2 \bar{V}_{--0}^3 + V_{+-0}^2 \bar{V}_{-+0}^3 - V_{0++}^2 \bar{V}_{0--}^3 - V_{0+-}^2 \bar{V}_{0-+}^3 \\
& + V_{0-+}^2 \bar{V}_{0+-}^3 + V_{0--}^2 \bar{V}_{0++}^3 - V_{-+0}^2 \bar{V}_{-+0}^3 + V_{-+0}^2 \bar{V}_{-+0}^3 \\
& + V_{++0}^3 \bar{V}_{--0}^2 + V_{++0}^3 \bar{V}_{--0}^1 + V_{+0+}^3 \bar{V}_{-0-}^1 + V_{+0-}^3 \bar{V}_{-0+}^1 \\
& - V_{-+0}^3 \bar{V}_{-+0}^2 + V_{-+0}^3 \bar{V}_{-+0}^1 + V_{0++}^3 \bar{V}_{0--}^2 + V_{0+-}^3 \bar{V}_{0-+}^2 \\
& - V_{0-+}^3 \bar{V}_{0+-}^2 - V_{0--}^3 \bar{V}_{0++}^2 + V_{-+0}^3 \bar{V}_{-+0}^2 - V_{-+0}^3 \bar{V}_{-+0}^1 \\
& - V_{-0+}^3 \bar{V}_{-0+}^1 - V_{-0-}^3 \bar{V}_{-0+}^1 - V_{--0}^3 \bar{V}_{++0}^2 - V_{--0}^3 \bar{V}_{++0}^1.
\end{aligned} \tag{S12}$$

The  $VV$  operator for the momentum mode  $\hat{k} = (1, 1, 1)$  is expressed as

$$\begin{aligned}
\mathcal{O}_{VV} = & -V_{+++}^1 \bar{V}_{---}^3 - V_{++-}^1 \bar{V}_{--+}^3 - V_{+-+}^1 \bar{V}_{-+-}^3 - V_{+--}^1 \bar{V}_{-++}^3 \\
& + V_{-++}^1 \bar{V}_{+--}^3 + V_{-+-}^1 \bar{V}_{+-+}^3 + V_{--+}^1 \bar{V}_{-+-}^3 + V_{---}^1 \bar{V}_{+++}^3 \\
& - V_{+++}^2 \bar{V}_{---}^3 - V_{++-}^2 \bar{V}_{--+}^3 + V_{+-+}^2 \bar{V}_{-+-}^3 + V_{+--}^2 \bar{V}_{-++}^3 \\
& - V_{-++}^2 \bar{V}_{+--}^3 - V_{-+-}^2 \bar{V}_{+-+}^3 + V_{--+}^2 \bar{V}_{-+-}^3 + V_{---}^2 \bar{V}_{+++}^3 \\
& + V_{+++}^3 \bar{V}_{---}^2 + V_{+++}^3 \bar{V}_{---}^1 + V_{++-}^3 \bar{V}_{--+}^2 + V_{++-}^3 \bar{V}_{--+}^1 \\
& - V_{+-+}^3 \bar{V}_{-+-}^2 + V_{+-+}^3 \bar{V}_{-+-}^1 - V_{+--}^3 \bar{V}_{-++}^2 + V_{+--}^3 \bar{V}_{-++}^1 \\
& + V_{-++}^3 \bar{V}_{+--}^2 - V_{-++}^3 \bar{V}_{+--}^1 + V_{-+-}^3 \bar{V}_{+-+}^2 - V_{-+-}^3 \bar{V}_{+-+}^1 \\
& - V_{--+}^3 \bar{V}_{-+-}^2 - V_{--+}^3 \bar{V}_{-+-}^1 - V_{---}^3 \bar{V}_{+++}^2 - V_{---}^3 \bar{V}_{+++}^1.
\end{aligned} \tag{S13}$$

## S2. The Parametrization of correlation functions

As for the decay process  $\eta_{c1} \rightarrow AB$ , we are interested in the following correlation function

$$C_{AB, \eta_{c1}}^{ij}(\hat{k}, t) \equiv \langle 0 | \mathcal{O}_{AB}^i(\hat{k}, t) \mathcal{O}_{\eta_{c1}}^{j, \dagger}(0) | 0 \rangle, \tag{S14}$$

where  $\mathcal{O}_{\eta_{c1}}^i$  is the interpolating operator that annihilates a  $\eta_{c1}$  state,  $\mathcal{O}_{AB}^i(\hat{k})(t)$  is any one of the two-particle operators defined in Eqs. (S4, S5, S7, S12, S13, S8, S9, S10) that annihilates a  $AB$  state with the same quantum number as that of  $\eta_{c1}$ . Actually, each term  $\mathcal{O}_{AB}^i(\vec{k})$  of the operator  $\mathcal{O}_{AB}^i(\hat{k})$  with a specifically oriented momentum  $\vec{k}$  and a specific index combination of  $\mathcal{O}_A$  and  $\mathcal{O}_B$  (if available),

$$\mathcal{O}_{AB}^i(\vec{k}) = \left[ \mathcal{O}_A(\vec{k}) \circ \mathcal{O}_B(-\vec{k}) \right]^i, \tag{S15}$$

contributes uniformly to  $C_{AB, \eta_{c1}}^{ij}(\hat{k}, t)$  by a quantity

$$C_{AB, \eta_{c1}}^{ij}(\vec{k}, t) \equiv \langle 0 | \mathcal{O}_{AB}^i(\vec{k}, t) \mathcal{O}_{\eta_{c1}}^{j, \dagger}(0) | 0 \rangle, \tag{S16}$$

with  $\vec{k}$  being the spatial momentum of  $A$  in the rest frame of  $\eta_{c1}$ . In Eq. (S15) the symbol ‘ $\circ$ ’ stands for the specific combination in the explicit expression of  $\mathcal{O}_{AB}^i(\hat{k})$  that results from Eq. (S1).

Let  $|A(\vec{k})B(-\vec{k})\rangle$  be the state generated by  $\mathcal{O}_{AB}^{i, \dagger}(\hat{k})$ , then in the space of  $|\eta_{c1}\rangle$  and  $|A(\vec{k})B(-\vec{k})\rangle$ , the temporal transfer matrix is expressed as

$$\hat{T} = e^{-a_t \hat{H}} = e^{-a_t \bar{E}} \begin{pmatrix} e^{-a_t \Delta/2} & a_t x_{AB} \\ a_t x_{AB} & e^{+a_t \Delta/2} \end{pmatrix}. \tag{S17}$$

where  $\bar{E} = (m_{\eta_{c1}} + E_{AB})/2$  and  $\Delta = m_{\eta_{c1}} - E_{AB}$  have been defined with  $E_{AB} = E_A + E_B$ . Note that this expression assumes the state normalizations  $\langle \eta_{c1} | \eta_{c1} \rangle = 1$  and  $\langle AB | AB \rangle = 1$ . Without losing the generality, in the following discussion we use the state normalization conditions

$$\begin{aligned}
\mathcal{N}_{\eta_{c1}} & \equiv \langle \eta_{c1}, \lambda | \eta_{c1}, \lambda \rangle \\
\mathcal{N}_{AB} & \equiv \langle AB; (\lambda' \lambda''), \vec{k} | AB; (\lambda' \lambda''), \vec{k} \rangle,
\end{aligned} \tag{S18}$$

where  $\lambda$  is the polarization index of  $\eta_{c1}$ , while  $\lambda'$  and  $\lambda''$  represent the the polarization indices (if available) for the final state mesons  $A$  and  $B$ , respectively. If we assume  $\mathcal{O}_{\eta_{c1}}^i$  does not couple to  $|AB\rangle$  states and  $\mathcal{O}_{AB}^i$  does not couple to the  $|\eta_{c1}\rangle$  state, then the  $\eta_{c1} - AB$  transition takes place at any time slice  $t' \in [0, t]$ , such that

$$\begin{aligned}
C_{AB,\eta_{c1}}^{ij}(t) &\sim \sum_{\lambda(\lambda'\lambda'')} \frac{1}{\mathcal{N}_{\eta_{c1}}\mathcal{N}_{AB}} Z_{AB,i}^{(\lambda'\lambda'')} Z_{\eta_{c1,j}}^{\lambda,*} \langle AB; (\lambda'\lambda''), \vec{k} | e^{-a_t \hat{H}t} | \eta_{c1}, \lambda \rangle \\
&\sim \sum_{\lambda(\lambda'\lambda'')} a_t x_{AB}^{(\lambda'\lambda'')\lambda} \frac{1}{\mathcal{N}_{\eta_{c1}}\mathcal{N}_{AB}} Z_{AB,i}^{(\lambda'\lambda'')} Z_{\eta_{c1,j}}^{\lambda,*}(\lambda) \sum_{t_1=0}^t e^{-a_t E_{AB}(t-t_1-1)} e^{-a_t m_{\eta_{c1}} t_1} \\
&\sim -\frac{\sinh(a_t \Delta t/2)}{\sinh(a_t \Delta/2)} e^{-a_t \bar{E}t} \sum_{\lambda(\lambda'\lambda'')} a_t x_{AB}^{(\lambda'\lambda'')\lambda} \frac{1}{\mathcal{N}_{\eta_{c1}}\mathcal{N}_{AB}} Z_{AB,i}^{(\lambda'\lambda'')} Z_{\eta_{c1,j}}^{\lambda,*} \\
&\rightarrow -t \left(1 + \frac{1}{24}(a_t \Delta t)^2\right) e^{-a_t \bar{E}t} \sum_{\lambda(\lambda'\lambda'')} a_t x_{AB}^{(\lambda'\lambda'')\lambda} \frac{1}{\mathcal{N}_{\eta_{c1}}\mathcal{N}_{AB}} Z_{AB,i}^{(\lambda'\lambda'')} Z_{\eta_{c1,j}}^{\lambda,*}, \tag{S19}
\end{aligned}$$

where  $x_{AB}$  is now replaced by the transition amplitude

$$x_{AB}^{(\lambda'\lambda'')\lambda}(\vec{k}) \approx \langle AB; (\lambda'\lambda''), \vec{k} | \hat{H} | \eta_{c1}, \lambda \rangle, \tag{S20}$$

with proper state normalizations,  $Z_{\eta_{c1,j}}^\lambda$  and  $Z_{AB,i}^{(\lambda'\lambda'')}$  are the overlapping matrix elements

$$\begin{aligned}
Z_{\eta_{c1,i}}^\lambda &= \langle 0 | \mathcal{O}_{\eta_{c1}}^i | \eta_{c1}, \lambda \rangle \equiv Z_{\eta_{c1}} \epsilon_\lambda^i(\vec{0}) \\
Z_{AB,i}^{(\lambda'\lambda'')} &= \langle 0 | \mathcal{O}_{AB}^i | AB; (\lambda'\lambda''), \vec{k} \rangle. \tag{S21}
\end{aligned}$$

The parametrization of  $Z_{AB,i}^{(\lambda'\lambda'')}$  is not so straightforward as that of  $Z_{\eta_{c1,i}}^\lambda$ . To the first order of the Bonn approximation, the two-particle state can be expressed as the direct product of the state vector of  $A$  and  $B$ , namely,

$$|AB; (\lambda', \lambda''), \vec{k}\rangle \approx |A, (\lambda'), \vec{k}\rangle \otimes |B, (\lambda''), -\vec{k}\rangle, \tag{S22}$$

such that  $\mathcal{N}_{AB}$  and  $Z_{AB,i}^{(\lambda'\lambda'')}$  are approximated by

$$\begin{aligned}
\mathcal{N}_{AB} &\approx \mathcal{N}_A \mathcal{N}_B \\
Z_{AB,i}^{(\lambda'\lambda'')} &\approx Z_A Z_B \epsilon_{(\lambda'\lambda'')}^i(\vec{k}, AB), \tag{S23}
\end{aligned}$$

where  $Z_A$  and  $Z_B$  are defined through

$$\langle 0 | \mathcal{O}_X^{(i)}(\vec{k}) | X; \lambda', \vec{k}\rangle = Z_X \epsilon_{(\lambda')}^i(\vec{k}) \tag{S24}$$

with  $X$  referring to  $A$  or  $B$ , and  $\epsilon_{(\lambda'\lambda'')}^i(\vec{k}, AB)$  is the polarization of  $AB$  defined by

$$\epsilon_{(\lambda'\lambda'')}^i(\vec{k}, AB) = \left[ \vec{\epsilon}_{(\lambda')}(\vec{k}) \circ \vec{\epsilon}_{(\lambda'')}(-\vec{k}) \right]^i. \tag{S25}$$

The meaning of the symbol “ $\circ$ ” here is the same as that in Eq. (S15). The brackets of the superscripts and subscripts mean that they are void for pseudoscalar mesons and the normal meanings for (axial) vector mesons. The factors  $Z_{\eta_{c1}}$ ,  $Z_A$  and  $Z_B$  are also encoded in the individual correlation functions of operators  $\mathcal{O}_{\eta_{c1}}$ ,  $\mathcal{O}_A^{(i)}(\vec{k})$  and  $\mathcal{O}_B^{(i)}(\vec{k})$  (no superscripts for pseudoscalar mesons),

$$C_{XX}^{(ii)}(t; \vec{k}) = \langle 0 | \mathcal{O}_X^{(i)}(\vec{k}, t) \mathcal{O}_X^{(i)\dagger}(\vec{k}, 0) | \rangle \rightarrow \frac{Z_X^2}{\mathcal{N}_X} \mathcal{P}_{ii}^X(\vec{k}) e^{-a_t E_X t}, \tag{S26}$$

where the normalization condition  $\mathcal{N}_X = 2E_X L^3$  is used for single particle states  $X = \eta_{c1}, A, B$ , and  $\mathcal{P}_X^{(ij)}$  is unity for pseudoscalars and

$$\mathcal{P}_X^{ij}(\vec{k}) = \sum_{\lambda} \epsilon_\lambda^i(\vec{k}) \epsilon_\lambda^{j*}(\vec{k}) = \delta_{ij} + \frac{k_i k_j}{m_X^2}, \tag{S27}$$

comes from the completeness of polarization vectors of (axial) vector mesons. Consequently, we have the ratio function

$$\begin{aligned}
R_{AB}(\vec{k}, t) &= \frac{C_{AB, \eta_{c1}}^{33}(\vec{k}, t)}{\sqrt{[C_{AA}(\vec{k}, t)C_{BB}(-\vec{k}, t)]^{33} C_{\eta_{c1}, \eta_{c1}}^{33}(\vec{0}, t)}} \\
&\approx t \left(1 + \frac{1}{24}(a_t \Delta)^2 t^2\right) \frac{1}{\sqrt{8L^3 m_{\eta_{c1}} E_A E_B}} \\
&\times \sum_{\lambda(\lambda' \lambda'')} \frac{a_t x_{AB}^{(\lambda' \lambda'') \lambda} [\epsilon_{(\lambda' \lambda'')}^3(\vec{k}, AB) \epsilon_{\lambda}^3(\vec{0})]}{\sqrt{\mathcal{P}_A(\vec{k}) \mathcal{P}_B(-\vec{k}) \mathcal{P}_{\eta_{c1}}^{33}(\vec{0})}} \quad (t \gg 1 \text{ and } (a_t \Delta)t \ll 1), \tag{S28}
\end{aligned}$$

which is free of the factors  $Z_{\eta_{c1}}$ ,  $Z_A$  and  $Z_B$ . It is easily seen that the transition amplitude

$$x_{AB}^{(\lambda' \lambda'') \lambda} \approx -\langle AB; \lambda' \lambda'', \vec{k} | \hat{H} | \eta_{c1}, \lambda \rangle \tag{S29}$$

can be derived from the slope of  $R_{AB}(\vec{k}, t)$  with respect to  $t$ .

In practice, we average contribution of Eq. (S16) over all the terms of  $\mathcal{O}_{AB}^i(\vec{k})$  to increase the statistics. The correlation functions of  $C_{AA}(\vec{k}, t)$  and  $C_{BB}(-\vec{k}, t)$  are also averaged accordingly.

## S2. Amplitudes

The two-body decay  $\eta_{c1} \rightarrow AB$  includes closed-charm decays  $\chi_{c1} \eta(\eta')$ ,  $\eta_c \eta(\eta')$ ,  $J/\psi \omega(\phi)$ , and open-charm modes  $D_{(s)}^* \bar{D}_{(s)}$ ,  $D_{(s)}^* \bar{D}_{(s)}$ ,  $DD_1(2420)$ , etc. The effective Lagrangian for closed-charm decays can be written as

$$\mathcal{L}_1^{\text{cc}} \sim -g_{\chi\eta} m_{\eta_{c1}} H_\mu A^\mu \eta - ig_{\eta_c \eta} H_\mu \eta_c \overleftrightarrow{\partial}^\mu \eta + iH_\mu \left( g\psi_\nu \partial^\nu \omega^\mu + g'\omega_\nu \partial^\nu \psi^\mu + g_0 \psi_\nu \overleftrightarrow{\partial}^\mu \omega^\nu \right), \tag{S30}$$

where  $\overleftrightarrow{\partial}$  represents  $\overleftarrow{\partial} - \overrightarrow{\partial}$ , and the fields  $H_\mu$ ,  $\chi_\mu$ ,  $\eta_c$ ,  $\eta$ ,  $\psi_\mu$  and  $\omega_\mu$  are for  $\eta_{c1}$ ,  $\chi_{c1}$ ,  $\eta_c$ ,  $\eta(\eta')$ ,  $J/\psi$  and  $\omega$  mesons, respectively. When the isospin doublet fields  $D_{1\mu}$ ,  $D_\mu$  and  $D$  are introduced for  $D_1$ ,  $D^*$  and  $D$  mesons of the flavor wave functions  $(|c\bar{d}\rangle, -|c\bar{u}\rangle)^T$ , the effective Lagrangian for open-charm decays reads

$$\begin{aligned}
\mathcal{L}_1^{\text{oc}} &\sim g_{D_1 D} m_{\eta_{c1}} H_\mu \frac{1}{2} \left( D_1^{\mu, \dagger} D + D^\dagger D_1^\mu \right) + g_{D^* \bar{D}^*} H^\mu \frac{i}{\sqrt{2}} \left( D^{\nu, \dagger} \partial_\nu D_\mu + \partial_\nu D_\mu^\dagger D^\nu \right) \\
&+ \frac{g_{D^* \bar{D}}}{m_{\eta_{c1}}} \epsilon^{\mu\nu\rho\sigma} (\partial_\mu H_\nu) \frac{1}{2} \left[ (\partial_\rho D_\sigma^\dagger) D - D^\dagger (\partial_\rho D_\sigma) \right]. \tag{S31}
\end{aligned}$$

According to the effective Lagrangian, the tree-level decay amplitudes read

$$\begin{aligned}
x_{AP}^{\lambda' \lambda} &= g_{AP} m_{\eta_{c1}} \vec{\epsilon}_\lambda(\vec{0}) \cdot \vec{\epsilon}_{\lambda'}^*(\vec{k}), \\
x_{PP}^\lambda &= 2g_{PP} \vec{\epsilon}_\lambda(\vec{0}) \cdot \vec{k}, \\
x_{VP}^{\lambda' \lambda} &= g_{VP} \vec{\epsilon}_\lambda(\vec{0}) \cdot (\vec{\epsilon}_{\lambda'}^*(\vec{k}) \times \vec{k}), \\
x_{D^* \bar{D}^*}^{\lambda' \lambda'' \lambda} &= 2g_{D^* \bar{D}^*} \vec{\epsilon}_\lambda(\vec{0}) \cdot \left( \vec{k} \times \left[ \vec{\epsilon}_{\lambda'}^*(\vec{k}) \times \vec{\epsilon}_{\lambda''}^*(-\vec{k}) \right] \right), \tag{S32}
\end{aligned}$$

where  $\vec{\epsilon}_\lambda(\vec{0})$ ,  $\vec{\epsilon}_{\lambda'}(\vec{k})$  and  $\vec{\epsilon}_{\lambda''}(-\vec{k})$  are the spatial components of the polarization vectors of the initial state  $\eta_{c1}$  and the vector mesons in the final state, respectively. As shown in Eq. (S32), the amplitude  $x_{AB}$  for the decay process  $\eta_{c1} \rightarrow AB$  is encoded in the ratio function  $R_{AB}(\vec{k}, t)$  and can be extracted from its slope in the time range where it behaves as a linear function. In the practical data analysis procedure,  $R_{AB}(\vec{k}, t)$  is fitted by the function form

$$R_{AB}(\vec{k}, t) = r_0 + r_1 t + r_3 t^3 \tag{S33}$$

and the fitted value of the parameter  $r_1$  is proportional to the amplitude  $x_{AB}$ . Before giving the numerical details of the extraction of  $r_1$ , we derive the explicit relation between  $r_1$  and the effective coupling  $g_{AB}$  mode by mode using Eq. (S32) as follows.

- **AP mode:** On our lattices, the mass thresholds of  $\chi_{c1}\eta_{(2)}$  and  $D_1\bar{D}$  are very close to  $m_{\eta_{c1}}$ , and the final AP states are in  $S$ -wave ( $L=0$ ), so we set  $\vec{k}=\vec{0}$ . According to the operator structure in Eq. (S4), one has

$$\begin{aligned}
r_1 &= \frac{1}{\sqrt{8L^3 m_{\eta_{c1}} E_A E_P}} \sum_{\lambda\lambda'} a_t x_{PA}^{\lambda'\lambda} \frac{\epsilon_{\lambda'}^3(\vec{k}) \epsilon_{\lambda}^{3*}(\vec{0})}{\sqrt{\mathcal{P}_{ii}^A(\vec{k}) \mathcal{P}_{jj}^{\eta_{c1}}(\vec{0})}} \\
&= \frac{g_{AP} m_{\eta_{c1}} a_t}{\sqrt{8L^3 m_{\eta_{c1}} E_A E_P}} \sum_{\lambda\lambda'} \frac{\epsilon_{\lambda'}^3(\vec{k}) \epsilon_{\lambda}^{3*}(\vec{0}) \epsilon_{\lambda}^{\mu}(\vec{0}) \epsilon_{\mu, \lambda'}^*(\vec{k})}{\sqrt{\mathcal{P}_{ii}^A(\vec{k}) \mathcal{P}_{ii}^{\eta_{c1}}(\vec{0})}}, \\
&= \frac{g_{AP} m_{\eta_{c1}} a_t}{\sqrt{8L^3 m_{\eta_{c1}} E_A E_P}} \frac{\delta_3^{\mu} (\delta_{\mu 3} + \frac{k_{\mu} k_3}{m_A^2})}{\sqrt{(1 + \frac{k_3^2}{m_A^2}) \cdot 1}} \\
&= \frac{g_{AP} m_{\eta_{c1}} a_t}{\sqrt{8L^3 m_{\eta_{c1}} E_A E_P}}.
\end{aligned} \tag{S34}$$

Or equivalently we have

$$g_{AP} = \frac{\sqrt{8L^3 m_{\eta_{c1}} E_A E_B}}{m_{\eta_{c1}} a_t} r_1. \tag{S35}$$

- **PP mode:** Similarly to the case of AP mode, for  $\vec{k} = \frac{2\pi}{La_s}(0, 0, 1)$  (the first term of Eq. (S8)), we have

$$r_1 = 2a_t g_{PP} \frac{1}{\sqrt{8L^3 m_{\eta_{c1}} E_P E_{P'}}} \sum_{\lambda} \frac{\epsilon_{\lambda}^i(\vec{0}) k_i \epsilon_{\lambda}^{3*}(\vec{0})}{\sqrt{\mathcal{P}_{33}^{\eta_{c1}}(\vec{0})}} = g_{PP} \frac{2k_3 a_t}{\sqrt{8L^3 m_{\eta_{c1}} E_P E_{P'}}}, \tag{S36}$$

where  $k^3$  is the  $z$ -component of  $\vec{k}$ . Finally we have

$$g_{PP} = \frac{\sqrt{8L^3 m_{\eta_{c1}} E_P E_{P'}}}{2k_3 a_t} r_1 \tag{S37}$$

- **VP mode:** The first terms of Eq. (S5), Eq. (S6), and Eq. (S7) give the same expression of  $r_1$

$$r_1 = \frac{1}{\sqrt{8L^3 m_{\eta_{c1}} E_V E_P}} \sum_{\lambda\lambda'} a_t x_{VP}^{\lambda'\lambda} \frac{\epsilon_{\lambda'}^1(\vec{k}) \epsilon_{\lambda}^3(\vec{0})}{\sqrt{\mathcal{P}_{11}^V(\vec{k})}} = \frac{g_{VP}}{\sqrt{8L^3 m_{\eta_{c1}} E_V E_P}} \frac{k_2 a_t}{\sqrt{1 + \frac{k_1 k_1}{m_V^2}}}, \tag{S38}$$

from which the effective coupling  $g_{VP}$  is determined through

$$g_{VP} = \sqrt{1 + \frac{k_1 k_1}{m_V^2}} \frac{\sqrt{8L^3 m_{\eta_{c1}} E_V E_P}}{k_2 a_t} r_1 \tag{S39}$$

- **VV mode:** Here we only consider the open-charm mode  $D^*\bar{D}^*$ , which must be in the  $L=1$  and  $S=1$  state. The first terms of Eq. (S11), Eq. (S13) and Eq. (S12) gives

$$r_1 = \frac{1}{\sqrt{8L^3 m_{\eta_{c1}} E_{D^*}^2}} \sum_{\lambda\lambda'\lambda''} a_t x_{D^*\bar{D}^*}^{\lambda'\lambda''\lambda} \frac{\epsilon_{\lambda'}^1(\vec{k}) \epsilon_{\lambda''}^3(-\vec{k}) \epsilon_{\lambda}^{3*}(\vec{0})}{\sqrt{\mathcal{P}_{11}^{D^*}(\vec{k}) \mathcal{P}_{33}^{\bar{D}^*} \mathcal{P}_{33}^{\eta_{c1}}(\vec{0})}}. \tag{S40}$$

Then for  $\vec{k} = \frac{2\pi}{La_s}(n, n, n)$ ,  $r_1$  is expressed as

$$r_1 = 2g_{D^*\bar{D}^*} k_1 a_t \left(1 + \frac{\vec{k}^2}{m_{D^*}^2}\right) \left(1 + \frac{k_1^2}{m_{D^*}^2}\right)^{-1}, \tag{S41}$$

For  $\vec{k} = \frac{2\pi}{La_s}(n, 0, 0)$  and  $\vec{k} = \frac{2\pi}{La_s}(n, n, 0)$ , one has

$$r_1 = 2g_{D^*\bar{D}^*} k_1 a_t \left(1 + \frac{\vec{k}^2}{m_{D^*}^2}\right) \left(1 + \frac{k_1^2}{m_{D^*}^2}\right)^{-1/2}. \tag{S42}$$

Thus, we obtain  $g_{D^*\bar{D}^*}$  at different momenta  $\vec{k}$ .

With the effective coupling  $g_{AB}$  determined from  $r_1$  for each decay mode, after averaging over the initial state polarization and the summation of the final state polarization, one can obtain the explicit expression of the decay amplitude squared

$$\overline{|\mathcal{M}(\eta_{c1} \rightarrow AB)|^2} = \frac{1}{3} \sum_{\lambda(\lambda'\lambda'')} |x_{AB}^{(\lambda'\lambda'')\lambda}|^2 \quad (\text{S43})$$

which enters calculation of the partial decay width directly

$$\Gamma_{AB} = \frac{1}{8\pi} \frac{k_{\text{ex}}}{m_{\eta_{c1}}^2} \overline{|\mathcal{M}(\eta_{c1} \rightarrow AB)|^2}, \quad (\text{S44})$$

where  $k_{\text{ex}}$  is the decay momentum determined by the experimental mass values of  $A$  and  $B$  along with a given  $m_{\eta_{c1}}$ , namely,

$$k_{\text{ex}} = \frac{1}{2m_{\eta_{c1}}} \lambda(m_{\eta_{c1}}^2, m_A^2, m_B^2)^{1/2} \equiv \frac{1}{2m_{\eta_{c1}}} (m_{\eta_{c1}}^4 + m_A^4 + m_B^4 - 2m_{\eta_{c1}}^2 m_A^2 - 2m_{\eta_{c1}}^2 m_B^2 - 2m_A^2 m_B^2)^{1/2}. \quad (\text{S45})$$

Specifically for the decay modes considered in this study, the explicit expressions of  $\overline{|\mathcal{M}|^2}$  are

$$\begin{aligned} \overline{|\mathcal{M}(\eta_{c1} \rightarrow AP)|^2} &= \frac{1}{3} g_{AP}^2 m_{\eta_{c1}} \left(3 + \frac{k_{\text{ex}}^2}{m_A^2}\right), \\ \overline{|\mathcal{M}(\eta_{c1} \rightarrow PP)|^2} &= \frac{4}{3} g_{PP}^2 k_{\text{ex}}^2, \\ \overline{|\mathcal{M}(\eta_{c1} \rightarrow VP)|^2} &= \frac{2}{3} g_{VP}^2 k_{\text{ex}}^2, \\ \overline{|\mathcal{M}(\eta_{c1} \rightarrow D^* \bar{D}^*)|^2} &= \frac{4}{3} g^2 k_{\text{ex}}^2 \frac{m_{\eta_{c1}}^2}{m_{D^*}^2}. \end{aligned} \quad (\text{S46})$$

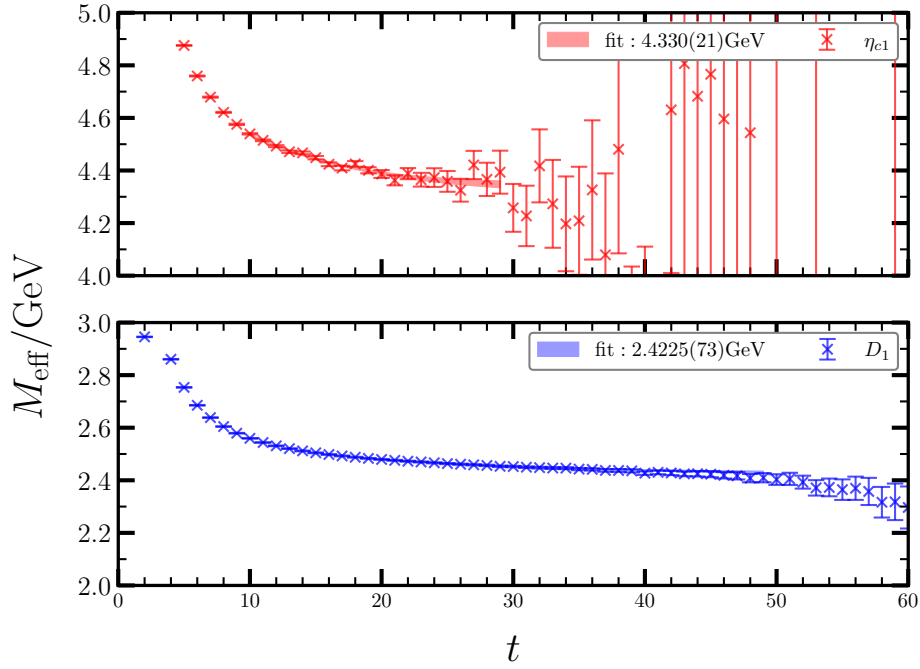


FIG. S1. The effective mass of  $1^{-+}$  charmoniumlike hybrid on L16 with fitting value  $m_{\text{eff}} = 4.330(21)$  MeV, and  $m_{\text{eff}} = 2.422(7)$  MeV for  $D_1$ .

### S3. Fitting details

As addressed in the main text, we use simple generic  $\bar{q}\Gamma q$  operators for all the single mesons, all of which are ground states of specific quantum numbers. In the framework of the distillation methods, quark fields are Laplacian Heaviside smeared such that the coupling of these operators to excited states are suppressed. In order to determine the energy of each meson  $X$  at a given momentum  $k = |\vec{k}|$ , we perform a two-mass fit to the correlation function  $C_X(k, t)$  through the function form

$$C_X(k, t) = W_1 \left( e^{-E_1(k)t} + e^{-E_1(k)(T-t)} \right) + W_2 \left( e^{-E_2(k)t} + e^{-E_2(k)(T-t)} \right), \quad (\text{S47})$$

with the second term accounting for the contribution from higher states. Indeed, this function form presents accurately for all the single mesons. In Fig. S1, the data points are the effective masses of  $\eta_{c1}$  (upper panel) and  $D_1$  (lower panel) on L16 ensemble. The shaded band in each panel illustrates the fit time range and the fit quality. The correlations of other single mesons (mainly pseudoscalars and vectors) have much better signal-to-noise ratios (except for  $\eta_{(2)}$ ).

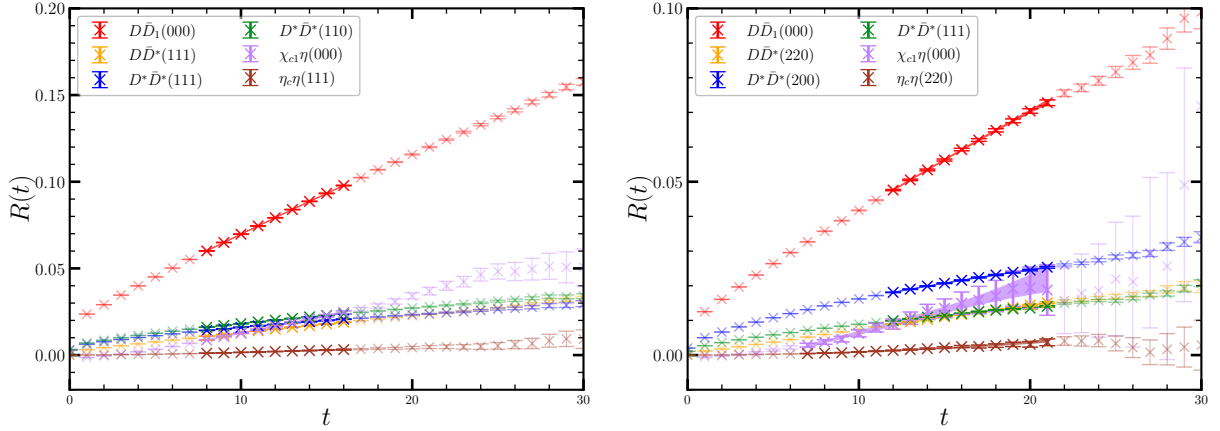


FIG. S2. The ratio function  $R_{AB}(\vec{k}, t)$  on the two gauge ensembles L16 (the left panel) and L24 (the right panel) for  $\eta_{c1} \rightarrow AB$ .  $AB$  refers to the decay modes  $D_1\bar{D}$ ,  $D^*\bar{D}$ ,  $D^*\bar{D}^*$ ,  $\chi_{c1}\eta_{(2)}$ ,  $\eta_c\eta_{(2)}$ . The shaded bands illustrate the fit results and the fit window using Eq. (S33).

For a two-body decay mode  $AB$  of  $\eta_{c1}$ , the magnitude of the relative momentum  $\vec{k}$  (denoted by the momentum mode  $\hat{k} = (n_1, n_2, n_3)$ ) is chosen to give the value of  $E_{AB} = E_A(\hat{k}) + E_B(\hat{k})$  as close to  $m_{\eta_{c1}}$  as possible. This is required for the derivation of Eq. (S19) and Eq. (S28). For some decay modes, more than one momentum modes are assumed to check the momentum dependence of the transition amplitude and the effective coupling. Table S1 lists the  $E_{AB}$  and  $a_t\Delta = a_t(m_{\eta_{c1}} - E_{AB})$  for all the meson-meson modes involved. As shown in Eq. (S28), the small values  $|a_t\Delta| \lesssim |0.01$  manifest that the derivation of  $R_{AB}(\vec{k}, t)$  from the linear behavior, depicted by  $(a_t\Delta)^2 t^2/24$ , is as small as 0.4% even at  $t = 30$ . Of course, the contamination from higher states will spoil the linear behavior, so we should fit  $R_{AB}(\vec{k}, t)$  using the function form of Eq. (S28) in a time range where the contribution of higher states is unimportant. Fig. S2 shows the  $t$ -behaviors of  $R_{AB}(\vec{k}, t)$  for all the decay channels concerned in this study. It is seen that the linear behavior does show up for each curve. The shaded curves illustrate the fit results and the fit time ranges using Eq. (S33). The fitted values of  $r_1$  and  $r_3$  are also shown in Table S1, where the absolute values of  $r_3$  are smaller than those of  $r_1$  by 3-4 orders of magnitude. Consequently, the fitted values of  $r_1$  are used to determine the final transition amplitude and the effective couplings. The fit stability of  $R_{AB}(\vec{k}, t)$  is also checked by varying the fit  $t$  window. In doing so, we fix the length of the fit window to be 10 and conduct the fit in the time range  $t \in [t_{\min}, t_{\min} + 10]$  by varying  $t_{\min}$  from 5 to 25. The  $\chi^2/\text{d.o.f}$  values and the values of  $r_1$  of the fits are illustrated in Fig. , where the left panels are the results of the L16 ensemble and the right ones are for the L24 ensemble. Obviously, the central values of  $r_1$  for all the decay modes are stable when  $t_{\min} > 7$ , while the errors increase with the increasing of  $t_{\min}$ . The smallness of the  $\chi^2/\text{d.o.f}$  values for all the fits manifest the feasibility of the function form in Eq. (S28). It is noted that the decay channels including isoscalar  $\eta$  has worse signal at  $t > 25$  due to the contribution of the light annihilation diagrams. We take the fitted values of  $r_1$  in the time ranges  $[t_{\min}, t_{\max}] = [8, 18]$  as our final results, and take  $\delta r_1 = (r_1^{(\max)} - r_1^{(\min)})/2$  of the fits with  $t_{\min} \in [6, 13]$  as a systematic error of  $r_1$  and add it to the statistical error in a quadratic way.

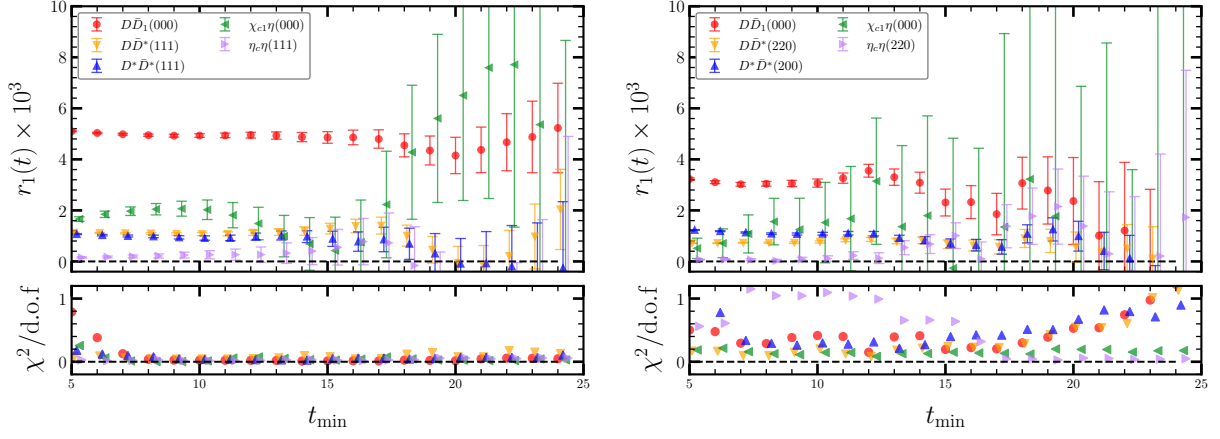


FIG. S3. The fit stability of varying our fit window selections on our  $r_1$  results. The horizontal axis, denoted  $t_{\min}$ , represents the case where we use the fit window  $[t_{\min}, t_{\min} + 10]$ .

TABLE S1. The energy  $E_{AB}$ ,  $a_t \Delta$  and the fitted  $r_1$  for the six decay modes. For each mode at a specific relative momentum mode  $(n_1 n_2 n_3)$ , the value of  $a_t \Delta = a_t (m_{\eta_{c1}} - E_{AB})$  is estimated by the central values of  $m_{\eta_{c1}}$  and  $E_{AB}$ .

Mode ( $AB$ )	$E_{AB}$ (MeV)	$a_t \Delta$	$r_0$	$r_1 (\times 10^{-3})$	$r_3 (\times 10^{-7})$
L16	$(m_{\eta_{c1}} = 4330(21) \text{ MeV})$				
$D\bar{D}_1(000)$	4304(7)	$\sim 0.004$	0.02077(38)	4.95(5)	-5.1(1.3)
$D\bar{D}^*(111)$	4301(4)	$\sim 0.004$	0.00210(19)	1.11(3)	-2.2(8)
$D^* \bar{D}^*(111)$	4405(10)	$\sim -0.011$	0.00702(25)	1.00(3)	-4.3(9)
$D^* \bar{D}^*(110)$	4288(4)	$\sim 0.006$	0.00702(25)	1.15(4)	-4.1(9)
$\chi_{c1} \eta_{(2)}(000)$	4262(8)	$\sim 0.010$	-0.0076(18)	2.04(26)	-0.9(6.8)
$\eta_c \eta_{(2)}(111)$	4347(39)	$\sim -0.003$	-0.00057(39)	0.20(6)	1.6(1.6)
L24	$(m_{\eta_{c1}} = 4328(68) \text{ MeV})$				
$D\bar{D}_1(000)$	4310(10)	$\sim 0.003$	0.0110(26)	3.10(26)	-3.3(3.5)
$D\bar{D}^*(220)$	4361(5)	$\sim -0.005$	-0.00027(69)	0.78(7)	-1.07(97)
$D^* \bar{D}^*(200)$	4269(2)	$\sim 0.009$	0.00598(87)	1.05(9)	-3.1(1.2)
$D^* \bar{D}^*(111)$	4216(3)	$\sim 0.016$	0.00234(62)	0.67(7)	-2.50(83)
$\chi_{c1} \eta_{(2)}(000)$	4260(7)	$\sim 0.010$	-0.0057(27)	1.18(38)	-3.0(9.0)
$\eta_c \eta_{(2)}(220)$	4304(25)	$\sim 0.004$	-0.00037(17)	0.10(3)	2.49(77)

The small but nonzero constant  $r_0$  can be understood as follows. Assuming the correlation function  $C_{AB, \eta_{c1}}^{33}(\vec{k}, t)$  in Eq. (S16) is contributed only from two orthogonal states  $|\eta_{c1}\rangle$  and  $|AB\rangle$  which are normalized as  $\langle \eta_{c1} | \eta_{c1} \rangle = 1$  and  $\langle AB | AB \rangle = 1$ , one has

$$C_{AB, \eta_{c1}}^{33}(\vec{k}, t) \equiv \langle 0 | \mathcal{O}_{AB}^i(\vec{k}, t) \mathcal{O}_{\eta_{c1}}^{j, \dagger}(0) | 0 \rangle = \langle 0 | \mathcal{O}_{AB}^3(\vec{k}, 0) \hat{T}^t \mathcal{O}_{\eta_{c1}}^{3, \dagger}(0) | 0 \rangle, \quad (\text{S48})$$

where  $\hat{T}$  is the transfer matrix defined in Eq. (S17) in the Hilbert space spanned by  $|\eta_{c1}\rangle = \begin{pmatrix} 1 \\ 0 \end{pmatrix}$  and  $|AB\rangle = \begin{pmatrix} 0 \\ 1 \end{pmatrix}$ .

For  $(a_t \Delta) \ll 1$  and  $(a_t x_{AB}) \ll 1$ , one has

$$\hat{T}^t = e^{-(a_t \hat{H})t} = e^{-(a_t \bar{E})t} \begin{pmatrix} e^{-(a_t \Delta)t/2} & (a_t x_{AB})t \\ (a_t x_{AB})t & e^{+(a_t \Delta)t/2} \end{pmatrix} + \mathcal{O}(a_t^2 t^2 \Delta x_{AB}). \quad (\text{S49})$$

Now considering

$$\begin{aligned} \mathcal{O}_{\eta_{c1}}^{3, \dagger} | 0 \rangle &= |\eta_{c1}\rangle \langle \eta_{c1} | \mathcal{O}_{\eta_{c1}}^{3, \dagger} | 0 \rangle + |AB\rangle \langle AB | \mathcal{O}_{\eta_{c1}}^{3, \dagger} | 0 \rangle \equiv \begin{pmatrix} Z_{\eta_{c1}}^{\eta_{c1}} \\ Z_{\eta_{c1}}^{AB} \end{pmatrix} \\ \mathcal{O}_{AB}^{3, \dagger} | 0 \rangle &= |\eta_{c1}\rangle \langle \eta_{c1} | \mathcal{O}_{AB}^{3, \dagger} | 0 \rangle + |AB\rangle \langle AB | \mathcal{O}_{AB}^{3, \dagger} | 0 \rangle \equiv \begin{pmatrix} Z_{AB}^{\eta_{c1}} \\ Z_{AB}^{AB} \end{pmatrix}, \end{aligned} \quad (\text{S50})$$

the correlation function  $C_{AB,\eta_{c1}}^{33}(\vec{k}, t)$  can be expressed as

$$C_{AB,\eta_{c1}}^{33}(\vec{k}, t) \approx Z_{AB}^{\eta_{c1}} (Z_{\eta_{c1}}^{\eta_{c1}} - Z_{\eta_{c1}}^{AB} (a_t x_{AB}) t) e^{-m_{\eta_{c1}} t} + Z_{AB}^{AB} (Z_{\eta_{c1}}^{AB} - Z_{\eta_{c1}}^{\eta_{c1}} (a_t x_{AB}) t) e^{-E_{AB} t}. \quad (\text{S51})$$

If  $\mathcal{O}_{\eta_{c1}}$  ( $\mathcal{O}_{AB}$ ) does not couple to  $|AB\rangle$  ( $|\eta_{c1}\rangle$ ), namely,  $Z_{\eta_{c1}}^{AB} = 0$  and  $Z_{AB}^{\eta_{c1}} = 0$ , then one can get the ratio function  $R_{AB}(\vec{k}, t)$  in Eq. (S28). However, if  $Z_{\eta_{c1}}^{AB}$  and  $Z_{AB}^{\eta_{c1}}$  are nonzero but small, one can easily derive that

$$R_{AB}(\vec{k}, t) \approx \left( \frac{Z_{\eta_{c1}}^{\eta_{c1}}}{Z_{AB}^{AB}} + \frac{Z_{\eta_{c1}}^{AB}}{Z_{\eta_{c1}}^{\eta_{c1}}} \right) - (a_t x_{AB}) t + \dots \rightarrow r_0 + r_1 t + \dots \quad (\text{S52})$$

Thus the constant term  $r_0 \sim \left( \frac{Z_{\eta_{c1}}^{\eta_{c1}}}{Z_{AB}^{AB}} + \frac{Z_{\eta_{c1}}^{AB}}{Z_{\eta_{c1}}^{\eta_{c1}}} \right)$  serves as a measure of the validity of the assumption

$$\langle 0 | \mathcal{O}_{\eta_{c1}} | AB \rangle \approx 0, \quad \langle 0 | \mathcal{O}_{AB} | \eta_{c1} \rangle \approx 0. \quad (\text{S53})$$

We list  $r_0$  of all the  $AB$  modes in Table S1, where one can see that all the values of  $r_0$  are less than 2%, justifying the above assumption. It's also noted that the slope  $r_1$  may substantiate a factor of  $\pm 1$  according to convention, and we have chosen to consider the positive  $r_1$  in this study.